GEOPHYSICAL STUDY OF NSUKKA AND UDI AREAS USING AEROMAGNETIC DATA

BY

EDEH, UJUNWA GLADYS

PG/M.Sc./14/68219

A Research work submitted in partial fulfilment of the Requirements for the Award of the Degree of Master of Science (M.Sc.) in

Solid Earth Geophysics

DEPARTMENT OF PHYSICS AND ASTRONOMY
FACULTY OF PHYSICAL SCIENCES

UNIVERSITY OF NIGERIA, NSUKKA

SUPERVISOR: DR D.N. OBIORA

AUGUST, 2016

TITLE PAGE

GEOPHYSICAL STUDY OF NSUKKA AND UDI AREAS USING AEROMAGNETIC DATA

CERTIFICATION

We hereby certify that this original work of the candidate Edeh Ujunwa Gladys (PG/MSC/14/68219) is accepted in partial fulfillment for the award of the degree of Master of Solid Earth Geophysics, Physics and Astronomy, Faculty of Physical Science, University of Nigeria Nsukka.

……………………..	**…………………..**
DR. D. N. OBIORA	**DATE**
(SUPERVISOR)	
……………………..	**…………………..**
PROF. J. O. URAMA	**DATE**
(HEAD OF DEPARTMENT)	
…………………………	**…...........................**
(EXTERNAL EXAMINER)	**DATE**

DEDICATION

This work is dedicated to Almighty God and to those who may find this work interesting.

ACKNOWLEDGEMENT

I wish to acknowledge God who made it possible for this work to be completed, may His name be highly exalted. Humbly wish to thank my supervisors Dr. P. O. Ezema and Dr D. N. Obiora for their active constructive criticism to make sure this thesis is a success, may God bless and keep them. I also wish to appreciate my family members; my parents (Chief and Mrs F. O. Edeh), my grandmother (Madam Rose Edenwani), my siblings (Ngozi Chukwunonyerem, Chinyere Edeh, Chioma Edeh, Ekene Edeh, and Chidiebere Edeh) for their countless support and goodwill, may God enlarge their coasts.

I cannot forget the loving gestures of my roommate Roseshirley Ohajikoba, her boyfriend Dr. Chuka Dominic Okoye, Sir Mike Nwakamma, my course mates; Abangwu Uchenna, Eneh Bethel, Ossai Okwudili, Ijeomah Chinedu, Okorie Chukwudi Alexius, Ekwueme Oliver and Bala Gabriel, my best friend Akpa Adaobi Ezenwaka, my lecturers, Dr Oha of Geology Department UNN, all the members of Catholic Association of Postgraduate Students (CAPS) UNN, St. Cecilia's Choir of Annunciation Outstation of St. Peter Chaplaincy UNN, members of Federation Theatre UNN, may favour and grace follow you all.

Finally I wish to acknowledge Mr Egbuhuzor, C. L., and Mr Mbamalu, C. J. for their ceaseless encouragement and kindness towards my happiness, may God almighty reward you all… Amen.

ABSTRACT

Aeromagnetic data of Nsukka and Udi areas were analyzed qualitatively and quantitatively. The study was aimed at mapping mineral deposits in sedimentary basin, delineating susceptibility of rocks in the area, dip, plunge and type of body causing the magnetic anomaly and their trends as well as estimating the depth to magnetic source bodies. Spectral Analysis, Source Parameter Imaging (SPI), and Forward and Inverse modelling methods were used in the quantitative interpretation. Regional- residual separation was applied to a total aeromagnetic intensity contour map to produce a residual aeromagnetic intensity contour map. Depth results from spectral analysis revealed two depth sources with the shallower magnetic sources varying from 314 to 1061 m with an average depth value of 632.3 m, whereas the depth of the deeper magnetic sources vary from 1465.9 to 5888.7 m with an average depth value of 3260.4 m. The SPI estimated depth ranges from 472.3 m (shallower magnetic bodies) to 6051.8 m (deeper magnetic bodies). The estimated depths from the forward and inverse modelling method are 6415 m, 2917 m, 3749 m, 1306 m, 4449 m and 2561 m for profiles 1 - 6 respectively, with respective susceptibility values of 0.0037, 0.0061, 0.0100, 0.0033, 0.0061 and 0.0100. These indicate the presence of sedimentary intrusions (shales), Quartzite, Hematite, Calcite and Quartz, which are typically sandstones and ironstones or oxides of iron that are magnetic in nature. The sedimentary cover in the area was generally high, thus will likely favour hydrocarbon generation.

TABLE OF CONTENTS

TITLE PAGE		i
CERTIFICATION		ii
DEDICATION		iii
ACKNOWLEDGEMENT		iv
ABSTRACT		v
TABLE OF CONTENTS		vi
LIST OF FIGURES		ix
LIST OF TABLES		xi
CHAPTER ONE: INTRODUCTION		1
1.1	Introduction	1
1.2	Geophysical Survey Methods	3
1.3	Types of Geophysical Survey	3
1.3.1	Seismic Methods	3
1.3.2	Electromagnetic Induction Method	4
1.3.3	Electrical Resistivity Method	5
1.4	Potential Field Methods	6
1.4.1	Gravity Method	6
1.4.2	Magnetic Method:	7
1.5	Location of the Study Area (Nsukka and Udi)	8
1.6	Geology of the Study Area	9

1.7 Purpose of Study 13

CHAPTER TWO: LITERATURE REVIEW 14

2.1 Reviews of Previous Study on Benue Trough and Anambra Basin 14

CHAPTER THREE: THEORY OF MAGNETIC METHOD 19

3.1 Overview of Theory of Magnetic Method 19

3.2 Magnetic Force Field 19

3.2.1 Magnetic Moment 21

3.2.2 Intensity of Magnetization 22

3.3 Total Magnetic Field B (Magnetic Induction) 22

3.3.1 Magnetic Susceptibility k 24

3.3.2 Causes of Magnetic Susceptibilities 24

3.4 Rock Magnetization 26

3.4.1 Mechanisms for Induced Magnetization: 27

3.4.2 Remanent Magnetism 28

3.5 The Earth Magnetic field 29

3.5.1 Magnetic Elements and their Characteristics 32

3.6 The Geomagnetic Field 33

3.6.1 Temporal variation of the earth's magnetic field 34

3.7 Aeromagnetic data and its interpretation 35

3.8 Magnetic anomalies 38

3.9 Methodology 38

3.10 Data preparation and processing: 39

3.11 Filtering techniques 40

3.12 Fourier transform 41

3.13 Spectral analysis 42

3.14 Source Parameter Imaging (SPI) 43

3.15 Forward and inverse modelling 44

3.16 Source of data 46

CHAPTER FOUR: RESULTS AND DISCUSSION 47

4.1 Qualitative map results 47

4.2 Quantitative interpretation of maps 52

4.2.1 Spectral Analysis 52

4.2.1.1 Plots of log of Energy and frequency 53

4.2.1.2 Estimation of Depth to Magnetic Sources 57

4.2.1.2.1Magnetic Basement Depth Map: 60

4.2.2 Source Parameter Imaging (SPI) 61

4.2.3 Forward and Inverse Modeling Results 62

4.3 Discussion of Result 67

CHAPTER FIVE: CONCLUSION AND RECOMMENDATION 70

5.1 Conclusion 70

5.2 Recommendation 71

REFERENCE 72

LIST OF FIGURES

Figure.1.1 Map of the study area 8

Figure 1.2 Stratigraphic Successions in the Anambra Basin (Nuhu, 2009) 11

Figure 1.3 Geological Map of Nsukka and Udi Area 12

Figure.3.1 A bar magnet illustrating lines of force (Dobrin and Savit, 1988) 20

Figure 3.2 A schematic representation of magnetic induction of a magnetic body showing the primary inducing field, , the induced magnetization, M, and the associated secondary field, Hs (Lelièvre, 2003) 11

Figure 3.3 Histogram showing susceptibilities of different rock types (Telford *et al*., 1990) 12

Figure.3.4 Illustrating the difference between the earth's geographic, geomagnetic and magnetic poles and the equator (McElhinny 1973) 30

Figure 3.5 Elements of the earth's magnetic component (Lowrie, 1997) 32

Figure 4.1 Map showing the TMI of the Study Area 49

Figure 4.2 Upward and Downward Continuation Map of the Study Area 49

Figure 4.3 First Vertical Derivative of the Study Area 50

Figure 4.4 First Horizontal derivative of the Study Area 50

Figure 4.5 Map Showing the Reduction to Pole 51

Figure 4.6 Residual Map of the Study Area 51

Figure 4.7 Showing the Regional Map of the Study Area 52

Figure 4.8 Map Showing Spectral Cell Division 53

Figure 4.9 Spectral plots of Log E against Frequency (rad/m) of cells 1 – 6 54

Figure 4.10 Spectral plots of Log E against Frequency (rad/m) of cells 7 – 12 55

Figure 4.11 Spectral plots of Log E against Frequency (rad/m) of cells 13 – 18 56

Figure 4.12 (a) Map of 2D Shallow Depth of Basement, (b) Map of 3D Shallow Depth of Basement 60

Figure 4.13 (a) Showing the 2D Shallow Depth of Basement, (b) Showing 3D Shallow Depth of Basement 61

Figure 4.14 SPI Grid Map 2D (a) and 3D (b) of the Study Area 62

Figure 4.15 Showing the TMI Curve with Profiles chosen 63

Figure 4.16 Model (Sphere) Result for Profile 1 64

Figure 4.17 Model (Sphere) Result for Profile 2 64

Figure 4.18 Model (Ellipsoid) Result for Profile 3 65

Figure 4.19 Model (Ellipsoid) Result for Profile 4 65

Figure 4.20 Model (Sphere) Result for Profile 5 66

Figure 4.21 Model (Cylinder) Result for Profile 6 66

LIST OF TABLES

Table 3.1 Magnetic Susceptibilities of Some Mineral (Telford *et al.*, 1990). 25

Table 4.1 Summary of the Log E/Frequency Graph for Deeper Slope 57

Table 4.2 Summary of the Log E/Frequency Graph for Shallow Slope 58

Table 4.3 Summary of Spectral Analysis Result 59

Table 4.4 Shows the Summary of Forward and Inverse Modeling Result. 67

CHAPTER ONE

INTRODUCTION

1.1 Introduction

Geophysical survey employing aeromagnetic method has become an essential and powerful tool for subsurface reconnaissance since it allows fast coverage of large areas and low cost per unit area explored, when compared with other geophysical methods. An aeromagnetic survey is a common type of geophysical survey carried out using a magnetometer aboard or towed behind an aircraft. The principle is similar to a magnetic survey carried out with a hand-held magnetometer, but allows much larger areas of the Earth's surface to be covered quickly for regional reconnaissance. The aircraft typically flies in a grid-like pattern with height and line spacing determining the resolution of the data (and cost of the survey per unit area). As the aircraft flies, the magnetometer records tiny variations in the intensity of the ambient magnetic field due to the temporal effects of the constantly varying solar wind and spatial variations in the Earth's magnetic field being due both to the regional magnetic field, and the local effect of magnetic minerals in the Earth's crust. By subtracting the solar and regional effects, the resulting aeromagnetic map shows the spatial distribution and relative abundance of magnetic minerals (most commonly the iron oxide mineral magnetite) in the upper levels of the crust.

Because different rock types differ in their content of magnetic minerals, the magnetic map allows a visualization of the geological structure of the upper crust in the subsurface, particularly the spatial geometry of bodies of rock and the presence of faults and folds. This is particularly useful where bedrock is obscured by surface sand, soil or water. Aeromagnetic data was once presented as contour plots, but now it is more commonly expressed as colored and shaded computer generated pseudo-topography images. The apparent hills, ridges and valleys are referred to as aeromagnetic anomalies. A geophysicist can use mathematical modeling to infer the shape, depth and properties of the rock bodies responsible for the anomalies.

Aeromagnetic surveys are widely used to aid in the production of geophysical maps and are also commonly used during mineral exploration. Some mineral deposits are associated with an increase in the abundance of magnetic minerals, and occasionally the sought after commodity may itself be magnetic (e.g. iron ore deposits), but often the elucidation of the subsurface structure of the upper crust is the most valuable contribution of the aeromagnetic data. Aeromagnetic survey is a powerful tool in delineating the regional geology (lithology and structure) and a detailed aeromagnetic map is proven to be very effective in cases where the geology of the studied area is clearly known (Hassanein and Soliman, 2008).

The aeromagnetic survey is the oldest potential field method used for hydrocarbon and minerals exploration. The aeromagnetic geophysical method plays a distinguished role when compared with other geophysical methods in its rapid rate of coverage and low cost per unit area explored. Onuba *et al.* (2008) pointed out that the main purpose of magnetic survey is to detect rocks or minerals possessing unusual magnetic properties that reveal themselves by causing disturbances or anomalies in the intensity of the earth magnetic field. The aeromagnetic survey is applied in mapping these anomalies in the earth's magnetic field and this is correlated with the underground geophysical structure. Faults usually show up by abrupt changes or close spacing in orientation of the contours as revealed by the magnetic anomalies. For minerals and intrusive, residual magnetic anomaly maps are useful since they identify the presence of intrusive, lava flows, or igneous plugs. It is believed that this project work will contribute to a better understanding of the geophysical structure of the area and it will provide a guide to future researchers.

1.2 Geophysical Survey Methods

Geophysical survey is the systematic collection of geophysical data for spatial studies. Detection and analysis of the geophysical signals forms the core of Geophysical signal processing. The magnetic and gravitational fields emanating from the Earth's interior hold essential information concerning magnetic and gravitational activities and the internal structure. As the Electromagnetic and gravitational waves are multi-dimensional signals, all the 1-D transformation techniques can be extended for the analysis of these signals. Geophysical surveys may use a great variety of sensing instruments, and data may be collected from above or below the Earth's surface or from aerial, orbital, or marine platforms. Geophysical surveys have many applications in geology, archaeology, mineral and energy exploration, oceanography, and engineering. Geophysical surveys are used in industry as well as for academic research.

1.3 Types of Geophysical Survey

We have different types of geophysical method which include; Seismic method, Electromagnetic Induction method, Electrical Resistivity method and Potential Field method.

1.3.1 Seismic Methods

Seismic method of exploration is the most versatile in geophysical methods. Gutenberg in his pioneering work on seismology raised heavy objects to some heights and allowed them to drop to the ground thereby causing earth tremor. With such tremor or explosion are associated with seismic waves of elastic strain energy that propagate outwards from the source. The seismic waves travel through the earth’s interior and the travel times are measured of waves that return to the surface after reflection or refraction at geophysical interfaces within the ground. The travel times may be converted into depth values to reveal the distribution of geological boundaries underneath. Seismic methods are used extensively by oil companies in the search for oil and gas. Shallow surveys for water table or investigation of foundation conditions for building are areas that seismic methods deal with. Seismic survey is carried out on land or sea and oil companies do offshore drilling after offshore geological surveys. In this method, it has fine detail, and good correlation to Geology. The seismic method measures the response of seismic (sound) waves that are input into the earth and then refract along or reflect off subsurface soil and rock boundaries. The seismic source is usually a sledgehammer blow to a metal plate on the ground, a larger weight drop, or an explosion. The earth response is measured by sensors called geophones, which measure ground motion. Two basic methods of seismic exploration are used; refraction and reflection.

Seismic Refraction: The seismic refraction method measures head waves that are refracted along geologic formations below the earth's surface. Refractions generally occur along the top of the water table and the uppermost bedrock formation. A plot of the arrival time of the first seismic wave to each geophone gives information about the depth and location of these geophysics horizons. This information is plotted in a cross section that shows the depth to the water table and to the first bedrock layer.

Seismic Reflection: The reflection method measures the time necessary for a sound impulse to travel from the source, bounce off a geophysics boundary, and return to the surface at a geophone. The reflection from a geologic horizon is similar to an echo off a cliff face.

1.3.2 Electromagnetic Induction Method

The electromagnetic induction (EM) method measures the response of an induced alternating current. A current is induced into the ground by a transmitting coil. A receiving coil is placed a short distance away to measure the induced earth current. The size of the induced current depends on the geologic material (lithology) beneath the transmitter and receiver. By mapping changes in the induced current, it is possible to map out changes in lithology, in order to determine the potential presence of an aquifer. The EM method is also very sensitive to metal. Thus, the location of buried metal objects, such as drums or pipes, can be mapped with this technique.

1.3.3 Electrical Resistivity Method

The resistivity imaging method uses standard arrays developed for electrical resistivity sounding and profiling techniques and modifies them to create two dimensional resistivity profiles. A line of electrodes is placed at equal intervals along the desired profile. Four electrodes are used at one time. Two inject current into the ground and two read the electrical potential between them. The resistivity meter and switch box automatically read many combinations of current and potential electrodes from short offsets to long offsets starting at one side of the electrode spread and moving toward the opposite end. The short offsets look at the shallow earth, and the longer offsets look more deeply.

One can typically use either the dipole-dipole or the Wenner-Schlumberger array. The dipole-dipole array gives good horizontal resolution, but may have a poor signal to noise ratio (S/N) because the potential electrodes are outside the current electrodes. The Wenner-Schlumberger array is more directed for vertical resolution, but it also gives reasonable horizontal resolution. This method has greater S/N than the dipole-dipole method because the potential electrodes are placed between the two current electrodes.

The field data contain apparent resistivity values and geometry information. These data are then inverted to produce a two dimensional (X - Z) plot of resistivity values. This resistivity inversion section is then used to interpret subsurface lithology.

1.4 Potential Field Methods

A field is a set of functions of space and time. We are concerned with two kinds of fields: Material fields and Force fields. Material Fields describe some property at a point of the material and at a given time (intensive quantity). Examples of such fields include; density, porosity, magnetic susceptibility, temperature, mass and heat. These are extensive quantities (depend on extent of material). Force fields describe forces that act at each point of space at a given time. Examples of force fields include; gravity, magnetic field and electrostatic field. Fields can be scalar or vector or tensor. A vector field can be described in terms of field lines (lines of flow, lines of force or flux lines). These are lines that are tangent at every point to the vector field.

Gravity and Magnetics also known as the "Potential Fields" methods are used in natural-resource exploration to help locate mineral, petroleum and groundwater resources. They are an indirect (above ground) means of sensing the density and magnetization (physical properties) of subsurface materials for the purpose of locating faults and other lithology. Potential-field surveys can cover large areas of ground quickly and inexpensively and are, therefore, often used to identify smaller target areas for further investigation.

1.4.1 Gravity Method

The gravity field is reassuringly simple, unipolar and almost perfectly vertical. The common unit of gravity measurement in exploration geophysics is milliGal (1,000 mGal = 1 Gal = 1 cm/s^2 = 0.01 m/s^2). These units refer to acceleration due to gravity, and the average value at the earth surface is around 980,000 mGal or 9.8 m/s^2. By comparison, anomalies in mineral and oil exploration seldom exceed a few hundred milliGals. Where the rocks underfoot are relatively dense and heavy, their extra gravitational attraction increases the downward pull and creates positive gravity anomalies ("gravity highs"). Where the rocks are light, the gravitational pull is diminished and the anomalies are negative ("gravity lows"). Gravity survey is the measurements of the gravitational field at a series of different locations over an area of interest. The gravity survey locates and describes the subsurface structures from the gravity effects caused by their anomalous densities (Lowrie, 1997). Gravity is useful wherever the formations of interest have densities that are appreciably different from those of surrounding formations. Some examples can be mapping sedimentary basins to deduce where sedimentary rocks consistently have lower density than basement rocks, salt bodies, that is, low density of salt, groundwater studies and burial chambers in pyramids.

1.4.2 Magnetic Method:

Magnetic survey is a geophysical survey technique that measures the magnetic field or its components at series of different locations over an area of interest, usually with the objective of locating concentrations of magnetic materials or of determining depth to basement. The technique requires the acquisition or measurement of the amplitude of the magnetic field at discrete points along survey lines distributed regularly throughout the area. Magnetic survey is useful whenever object of investigation has a contrast in magnetic susceptibility or remanence. Visible example includes, mapping structure on basement, mapping sedimentary basins and direct location of ores containing magnetite. The purpose of magnetic surveying is to identify and describe regions of the Earth's crust that have anomalous magnetizations. In the realm of applied geophysics, these anomalous magnetizations might be associated with local mineralization that is potentially of commercial interest, or they could be due to subsurface structures that have a bearing on the location of oil deposits. In global geophysics, magnetic surveying over ocean ridges provided vital clues that led to the theory of plate tectonics and revealed the polarity history of the Earth's magnetic field since the Early Jurassic.

1.5 Location of the Study Area (Nsukka and Udi)

Nsukka area lies between latitudes 6°30´ and 7°00´ North and longitudes 7°00´ and 7° 30´ East in the southeastern geopolitical zone of Nigeria and Northern part of Enugu state. It is bounded in the North by Benue state and in the East by Ebonyi state and covers a total surface area of approximately 3,961 square kilometers. Udi area lies between latitude of 6°19′ and 7°00′ North and longitudes 7°26′ and 7°30′E. The average elevation of Udi area is 437 meters. It has an area of 897 km² and a population of 234,002 at the 2006 census. Hence it can be inferred that the study area lies between Latitude 6°00′ N– 7°00′N and Longitude 7°00′E – 7°30′E. Figure 1.1 shows the Map of the Study Area.

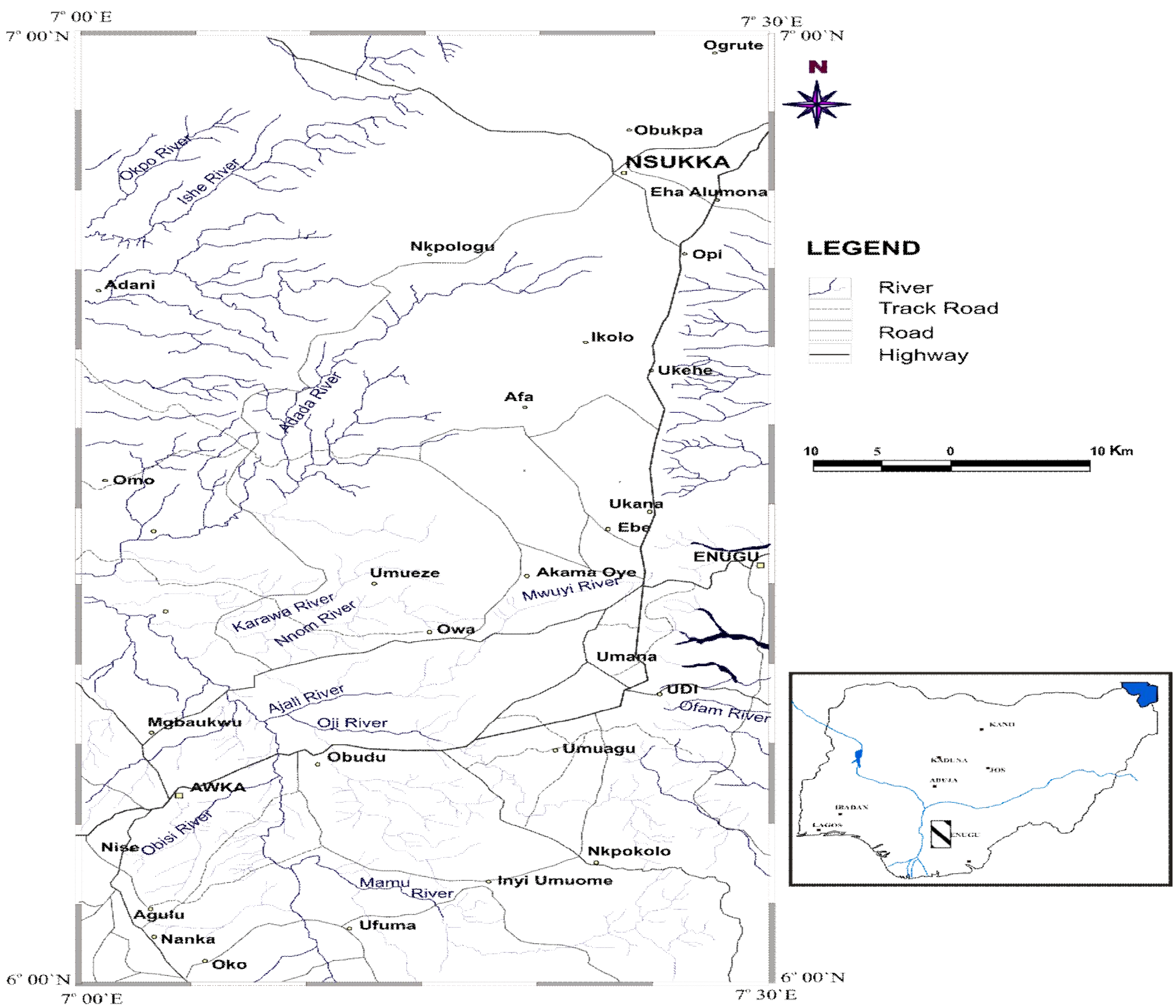

Figure 1.1: Map of the study area

1.6 Geology of the Study Area

The study area (Nsukka and Udi) is a sedimentary Basin within the Anambra Basin underlain by rocks which range in age from Coniacian to Paleocene. Anambra Basin consist of six major rock formations namely Nkporo Formation including Enugu Shale of Campanian, Agwu shale, Mamu formation, Ajali formation, Nsukka formation and Imo shale formation. These rocks are grouped into four formations namely: Mamu formation, Ajali Sandstone, Nsukka Formation, and Imo Shale Formation (Nwajide and Reijers, 1995; Onwuemesi, 1995). Sediments deposited within this time interval occur in four distinct physiographic provinces, namely the Cross River plains, the Escarpment, the Plateau and the Anambra Plains. It was discovered that over 3,965 m of sediments comprising shales, sandstones, limestone and coal were deposited in the area. Their environment of deposition varied from marine, through brackish water to entirely continental. Some of these sediments are of considerable economic importance and contain reserves of coal, natural gas, glass sands and considerable prospects for liquid hydrocarbon. The soil is rich and sustains a virile rural agriculture. The highest point in the area is about 590 m above datum plane but the lowlands generally have heights below 250 m above sea level. There are several elongated and conical hills separated by dry and wet valleys. The geology of Nsukka and Udi environs are composed mainly of Imo Formation of Paleocene, Nsukka Formation, Ajali Formation of Maastichtian and Mamu Formation (Nwajide and Reijers, 1995; Onwuemesi, 1995). Figure 1.2 is a typical Stratigraphic succession in Anambra Basin, while figure 1.3 shows the geological map of the study area.

Nkporo Formation: The Nkporo shale is the basal sedimentary unit that was deposited following the Santonian folding and inversion in Southeastern Nigeria and indicates a late Campanian age, based on the presence of Afrobolivina afra. The formation is generally poorly exposed but has been described as coarsening upward deltaic sequence of shale and interbed of sands and shale with occasional thin beds of limestone.

Agwu Shale Formation: This formation constitutes the oldest rocks exposed in the area and represent sediments deposited towards the terminal phase of the Turonian transgressive cycle. The contact with underlying Eze-Aku Shale Formation (Turonian) does not occur within the map area, but this is known to be conformable (Nwachukwu 1972). Agwu shale Formation is approximately 900 meters thick and comprises well bedded bluish grey shale with thin fine-grained sandstone, calcareous sandstone and occasional limestone members.

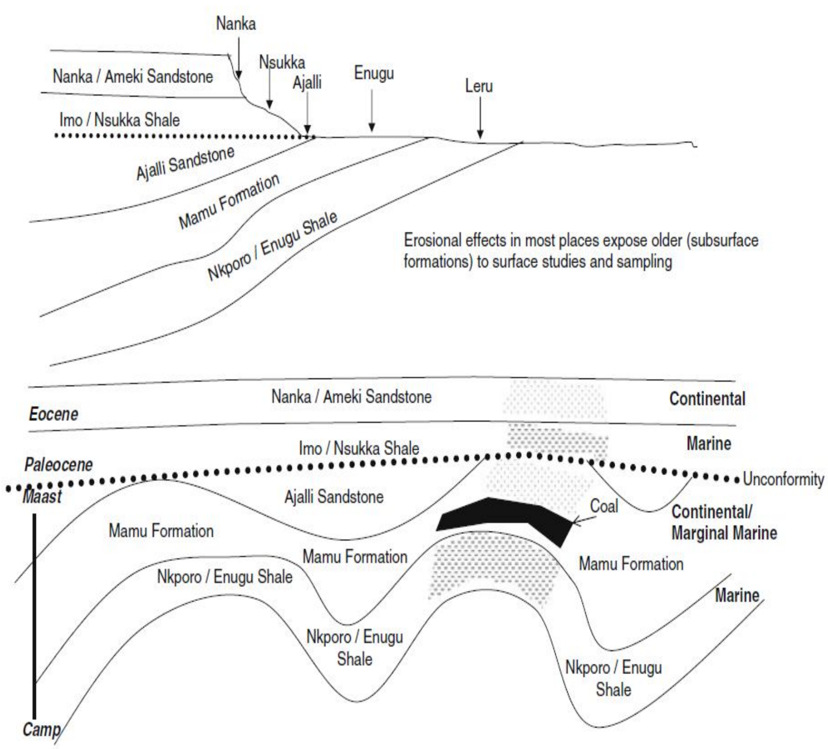

Figure 1.2: Stratigraphic Successions in the Anambra Basin (Nuhu, 2009)

The Enugu Shale: The Enugu shale is restricted to the central and northern parts of the Anambra Basin and consists of carbonaceous grey black shales and coals with interbeds of very fines and sandstone/siltstone deposited in lower flood plain and swampy environment.

The bedding planes are poorly defined with early diagenetic minerals such as pyrite and siderites. The sediments have a poorly developed foreshore and shoreface with extensive coastal swamps. The Enugu shale was assigned Campanian to Lower Maastrichtian, based on diagenetic species of palynomorphs such as Cingulatisporites ornatus and Tricolpites tienebaensis (Reyment, 1965; Whiteman, 1982).

The Owelli Sandstone: The Owelli sandstone regarded as a facies of the Nkporo groups is a lateral equivalent of Enugu shale. It is an elongate shoestring sand body to the northwest defining a meander belt of fluvial channel system and a fluviatile point bar. The Enugu and Owelli sandstone were deposited in open marine shelf and alternatively storm and tide dominated.

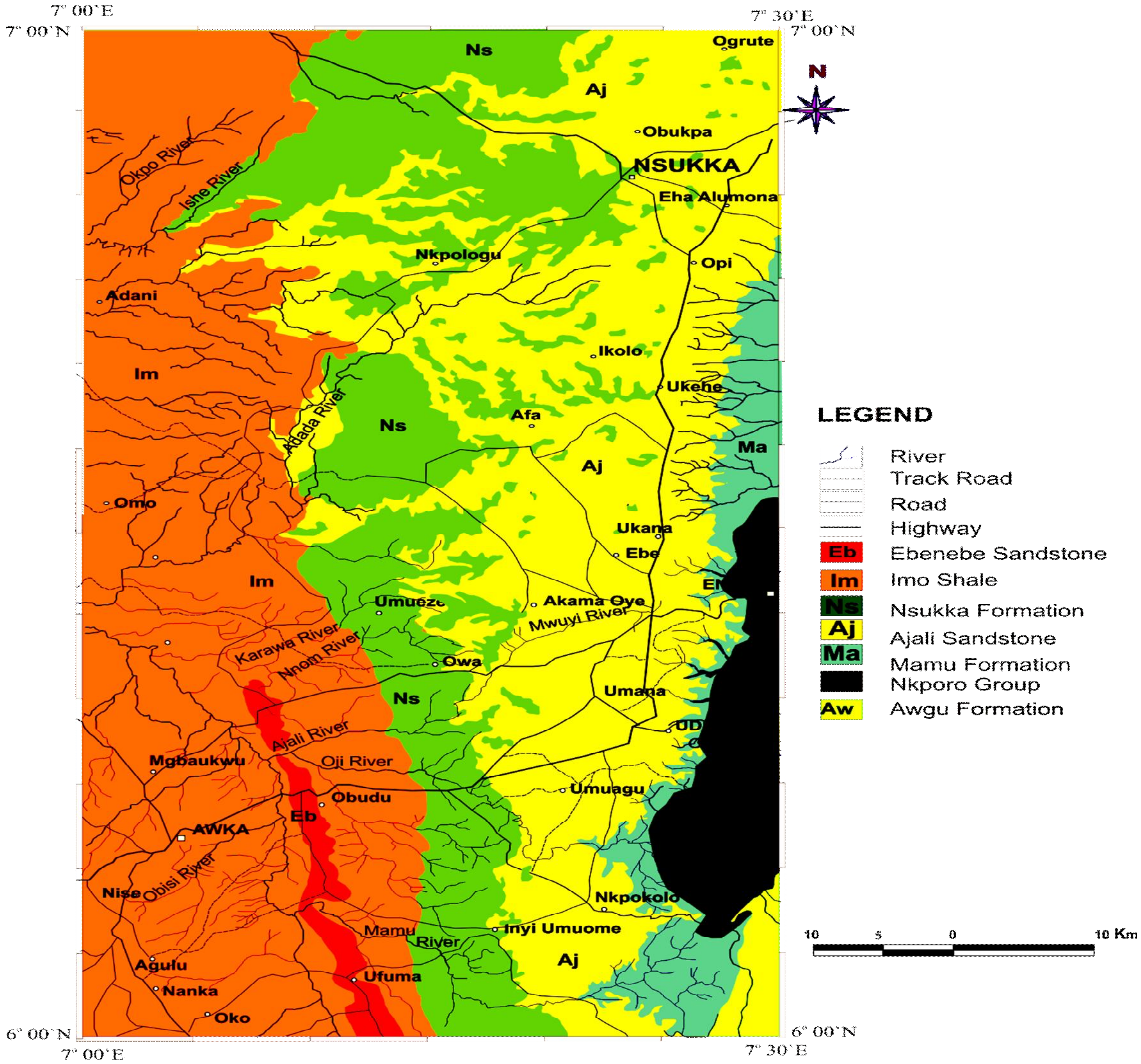

Figure 1.3: Geological Map of Nsukka and Udi Area

The Owelli sandstone is typically massive, hard and often ferruginous in some places and friable, it may be prominently cross bedded, medium-coarse grained with pebbles, sometimes aligned at the base of the cross beds.

Mamu Formation: The mamu formation overlies the Enugu shale conformably and contains sandstone, shale sandstone, sandy-shale with coal seams in various horizons (Reyment, 1965). The sediments pile varies across the basin and ranges from 75 m to over 1000 m (Reyment, 1965; Ladipo *et al.*, 1992). The possible environments of deposition are estuarine flood plain, swamp and tidal flat flood plain. It is excellently exposed along the Enugu-Onitsha road at the Millken Hill and the outskirts of Enugu (Kogbe, 1974). The age of this formation is put at lower-middle Maastrichtian and has a significant thickness variation from about 100 m in the south to as much as 100 m in the central and northern part of the basin (Ladipo *et al.*, 2001).

Ajali Sandstone: The Ajali sandstone overlies the Mamu Formation and has a diachronous age from South to North (Middle-upper Maastrichtian) and exhibits significant thickness variation from less than 300 m to over 1000 m at the centre of the basin (Ladipo *et al.*, 2001). Depositional characteristics are uniform for most parts of the basin, made up with textually mature sand facies i.e. mature quartz arenite intercalated with kaolinite beds. Dominant sedimentary structures are cross bedding associated with reactivation surfaces, mud drapes, tidal bundles, backflow ripples, channel cut and fills and lateral accretion surface (Ladipo *et al.*, 1992).

1.7 Purpose of Study

The main aim of this study is to interpret qualitatively and quantitatively the aeromagnetic data of Nsukka and Udi areas in southeastern Nigeria. The objectives of the interpretation include the determination of:

i. Susceptibility values of rock types in the area
ii. Thickness of the sedimentary basin
iii. Depth of the anomalous bodies
iv. Dip, plunge and type of body causing the magnetic anomaly
v. Mineralization of the area

CHAPTER TWO

LITERATURE REVIEW

2.1 Reviews of Previous Study on Benue Trough and Anambra Basin

The search for mineral deposits and hydrocarbon has been a major business challenge in Nigeria right from pre-colonial era till date. As the hydrocarbon potentials of the prolific Niger Delta becomes depleted or in the near future may be exhausted due to continuous exploitation, attention needs to be shifted to other sedimentary Basins. The lower Benue Trough, Anambra basin in particular, is one of those Basins being suspected to have high hydrocarbon potential, besides other economic mineral deposits concentration (Obiora *et al*., 2015). The origin and evolution of the Benue Trough of Nigeria is fairly documented (Wright, 1976; Petters, 1978; Ofoegbu, 1985). Generally, the Benue Trough is believed to have been formed when the South America separated from Africa (Petters, 1978). The major component units of the Lower Benue Trough include the Anambra Basin, the Abakaliki Anticlinorium and the Afikpo Syncline.

The investigation carried out in the Lower Benue Trough (precisely in the Abakaliki Anticlinorium) by Ehinola *et al*. (1985) revealed that mid – cretaceous oil shale deposits have been discovered in the Abakaliki Basin of the Lower Benue Trough of Nigeria. The oil shale was named 'Lokpanta oil shale' based on outcrops in Lokpanta town situated near Awgu in southeastern Nigeria. On contrary, Nwachukwu (1975), who studied inclusions found minerals from the area, estimated from his results that temperatures in the range of 100 – 160^{o}C prevailed during the formation of those minerals. This agrees with Whiteman (1982) and others who argues that the history of the Abakaliki Anticlinorium makes it unlikely to be a good hydrocarbon province. Ajakaiye (1981) and Ofoegbu (1984, 1985, 1988), by their analysis of both ground and airborne magnetic data over the Benue trough have shown extensive block faulting in the trough. These faults in places attain considerable lengths and mark out several basined structures in the trough. According to Onwuemesi (1997), who used one dimensional spectral analysis of aeromagnetic anomalies and curie depth isotherm in Anambra basin of Nigeria, states that sedimentary thickness (depth to the basement) in the Anambra Basin which is part of the Lower Benue Trough varies between 0.9 and 5.6 km, while the depth to Curie temperature isotherm varies between 16 and 30 km below the mean sea level. Onu *et al*. (2011) using spectral analysis to interpret the aeromagnetic data over the lower Benue Trough and some adjoining areas, stated that depths to magnetic source bodies in the Lower Benue Trough and some adjoining areas vary from 0.518 to 8.65 km with a mean depth of 3.513 km (for deeper magnetic source bodies) and 0.235 km to 3.91 km with a mean depth of 1.389 km (for shallow magnetic sources). Wright *et al*. (1985) states that the minimum thickness of the sediment required for the commencement of oil formation from marine organic remains would be 2.3 km.

Obiora *et al*. (2015) agrees that the Benue Trough of Nigeria is one of the major tectonic features in West Africa. It is an elongated rifted depression that trends NE-SW from the south, where it merges with the Niger Delta, to the north, where its sediments are part of the Chad Basin successions. The Benue Trough attains an approximate length of 800 km. It has a width of 130 to 150 km and is filled with Cretaceous sediments whose ages range from Middle Albian to Maestrichtian. Their thickness varies from about 6 km in the Lower Benue to about 5 km in the Upper Benue. Okeke (1992) carried out work on comparison of graphical methods of magnetic interpretation based on the interpretation of aeromagnetic anomaly profiles across the lower Benue Trough. The results of the work confirm the usefulness of some graphical methods of magnetic interpretation particularly when applied to isolated and non – interfering anomalies. In this study an entirely different method is employed rather than graphical method.

Ofoegbu (1984) interpreted the aeromagnetic anomalies over the Lower and Middle Benue Trough in terms of basic intrusive bodies which may occur either within the Cretaceous rocks or within the basement or both. He obtained a depth ranging from 0.5 to 7 km in the lower and middle Benue Basin and concluded that, although some of the observed anomalies could be attributed to the basement underneath the Benue Trough, the magnetic anomalies could not be satisfactorily interpreted fully in terms of a basement of variable topography. In the work of Igwesi and Umego (2013), they interpreted the aeromagnetic anomalies over some part of lower Benue Trough, using Spectral analysis which indicated a two layer source model with depth for deeper magnetic source ranging from 1.16 to 6.13 km with average of 3.03 km and depth to the shallower magnetic source ranging from 0.016 to 0.37 km with average of 0.22 km. Onuba *et al.* (2011) interpreted the aeromagnetic anomalies over Okigwe area and estimated the depth to basement using slope methods. They established two depth models varying from 2.18 to 4.91 km for deeper sources, while the shallower sources vary from 0.55 to 1.82 km. However, they did not recommend hydrocarbon exploration in the area since the area has low thickness of sediments on the average. Adetona and Abu (2013) estimated the thickness of sedimentation within the Lower Benue Basin and Upper Anambra Basin. They employed spectral depth analysis which used the radial average energy spectrum to obtain a depth of 7.3 km and source parameter imaging to obtain a depth of 9.847 km. Hence the research shows that the maximum depth of sedimentation within the Anambra basin is approximately 10 km and is high enough for the attainment of temperatures of approximately 60°C and higher than is required for thermal degradation of kerogen yielding hydrocarbons.

Ezema *et al.* (2014) used only forward and inverse modeling to interpret the aeromagnetic data of Abakaliki which showed maximum depths of 4.96 to 9.8 km with minimum depths ranging from 0.12 to 0.17 km. Likkasson *et al.* (2005) used directional filtering and spectral analysis in the lower and middle Benue basin and obtained spectral matching yielding three dipoles equivalent source layers at 0.89 km to 4.33 km and 18.22 km where 4.33 km corresponds to maximum thickness within middle Benue basin. Obi *et al.*, (2009) interpreted the aeromagnetic modeling of subsurface intrusive and its implication on hydrocarbon evaluation of the lower Benue trough of Nigeria. Twelve intrusive bodies were obtained which ranged from 1.0 km to 40 km. Depth was estimated based on SAKI modeling, power spectrum and horizontal gradient magnitude which showed sediment thickness in the range of 1.0 km to 40 km.

Obiora *et al.* (2015) interpreted aeromagnetic data of Nsukka area qualitatively and quantitatively. They employed standard Euler deconvolution, Source Parameter Imaging (SPI), Forward and Inverse modeling techniques in their quantitative interpretation with the aim of determining depth/thickness of the sedimentary Basin, magnetic susceptibilities and type of mineralization prevalent in the area. They did not employ spectral analysis and their study concentrated only at Nsukka area. They did not include Udi area in their study. Oasis montaj 6.4.2 software and potent Q 4.10.07 software were employed in their data analysis. Their result of Forward and inverse modeling estimated depths for profiles 1, 2, 3, 4 and 5 were 1644, 2285, 1972, 2193 and 1200 m respectively, with respective susceptibility values of 0.0031, 0.0073, 1.4493, 0.0069 and 0.0016 which indicate dominance of iron rich minerals like limonite, hematite, pyrrhotite and pyrite, and forms lateritic caps on sandstones. Results from their SPI estimated depth ranges from 151.6 m (outcropping and shallow magnetic bodies) to 3082.7 m (deep lying magnetic bodies). Depths of shallow magnetic sources resulting from lateritic bodies in the outcrops within their study area as estimated by Euler depths for the four different structural index (SI = 0.5, 1, 2, 3) ranges from 7.99 to 128.93 m. They concluded that 35 to 150 m depth are good potential water reservoirs for Nsukka and environs and depths of 1644 to 3082.7 m show sufficiently thick sediments suitable for hydrocarbon accumulation.

Ikpokonte and Ajayi (2003) used a preliminary interpretation of shallow regional structures deduced from ground magnetic data over the eastern part of the lower Benue trough (confluence) area, Nigeria to investigate the anomalies found in the regions. He postulated that the NE – SW trending anomalies in the region are thought to be possibly associated with the basement ridge which occur within and are parallel to the ground trend of the Benue trough. The gravity anomaly models on the profiles he produced also show that these ridges may also be intruded in places by intra basement basic bodies. Thus they arrived to a conclusion that the lower Benue trough is underlain by basic intrusive under uplifted basement at its north and south margins and under the deep basin. As such, the basement of this basin is irregular and forms a step fault at the margins and sub – basins at the depth. This characterizes the trough in terms of deep lying basement and highly magnetic intrusive bodies either within the sediments or basement or both. Sharma (1987) concluded that of all geophysical methods, mapping is the oldest, simplest, most reliable and widely used technique for locating both hidden ores and structures associated with mineral deposits.

These studies were carried out within the Lower Benue Trough in which Nsukka and Udi areas fall. Among these studies only one was carried out specifically in Nsukka area, but none in Udi area. Source Parameter Imaging (SPI), Euler deconvolution and Modeling techniques were employed in determining the magnetic anomalies in Nsukka area, but Spectral Analysis was not employed.

CHAPTER THREE

THEORY OF MAGNETIC METHOD

3.1 Overview of Theory of Magnetic Method

The earth's magnetic field dominates most magnetic measurements made at or near the surface of the Earth. The Earth's total field intensity varies considerably by location over the surface of the Earth. Most material except for permanent magnets, exhibit an induced magnetic field due to the behavior of the material when the material is in a strong field such as the Earth's. Induced magnetization (sometimes called magnetic polarization) refers to the action of the field on the material wherein the ambient field is enhanced causing the material itself to act as a magnet (Wightman *et al.* 2003).

3.2 Magnetic Force Field

Magnetic field of the Earth is measured because geologic structures (like ore bodies or faults) often produce a small magnetic field that distorts the main magnetic field of the Earth. These anomalies can be detected by measuring the magnetic field near the surface of the ground. By analyzing these measurements, geophysicist can learn about geophysical structures even though the structures may be concealed entirely below the Earth's surface. Magnetic measurements are usually made from low-flying airplanes flying along closely spaced parallel flight lines. Additional flight lines are flown in the perpendicular direction to assist in data processing. These huge volumes of measurements are then processed into a digital aeromagnetic map. Assisted by computer programs, the geophysicists build a geophysical interpretation from the digital aeromagnetic data. Interpretations often involve map-based information (e.g. a fault map) and a three dimensional information (e.g. a geophysical cross section).

In magnetic surveys, one of the most important tools in modern geophysical mapping is the use of aeromagnetic surveys. They are fast and provide a great deal of information about the distribution of rocks occurring under thin layers of sedimentary rocks. Magnetic force is similar to the force that exists between two point charges as stated by Coulombs in 1985. Coulombs showed that the force of attraction or repulsion between two electrically charge bodies and between magnetic poles (dipoles) also obey an inverse square law like that was derived for gravity by Newton. Therefore magnetic force is the actual force exerted between two magnetic poles. Figure 3.1 shows a bar magnet illustrating lines of force.

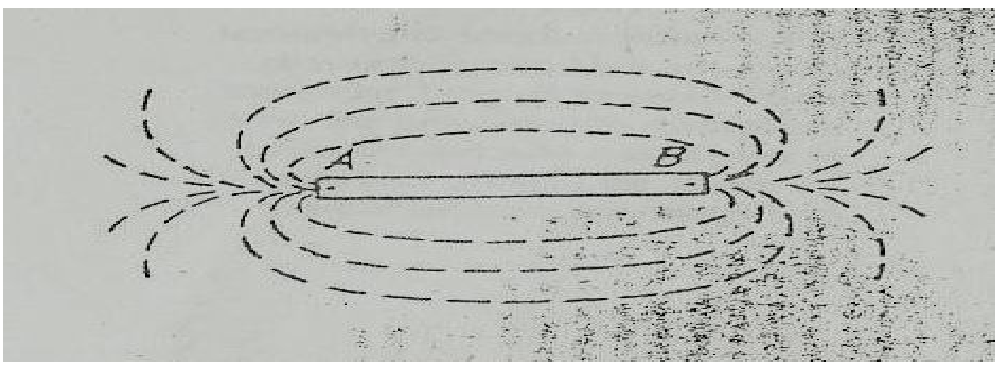

Fig 3.1: A bar magnet illustrating lines of force (Dobrin and Savit, 1988).

Mathematically, magnetic force is stated in Coulomb's law as (Telford *et al.*, 1990);

$$F = \left(\frac{P1P_2}{\mu r^2}\right) r_1 \tag{3.1}$$

where μ is the constant of proportionality known as magnetic permeability, P_1 and P_2 are the strength of the two magnetic monopoles and r is the distance between the two poles. Permeability μ is used to describe the magnetic property of the material in which the poles are situated and r_1 is the unit vector directed from P_1 towards P_2. Unlike the gravitational constant G, the magnetic permeability, μ, is a property of the material in which the two monopoles, P_1 and P_2, are located. If they are in a vacuum, μ is represented as μ_0 which is called the magnetic permeability of free space.

Unlike M_1 and M_2 as in gravitational force expression, P_1 and P_2 can be either positive or negative in sign. If P_1 and P_2 have the same sign, the force between the two monopoles is repulsive. If P_1 and P_2 have opposite signs, the force between the two monopoles is attractive.

Magnetic permeability μ is a dimensionless constant that describes the magnetic property of the material in which poles are situated. It is the measure of the ability of a magnetic material to support the formation of a magnetic field within itself. It is measured in Newton-per ampere squared.

Magnetic Field Strength H: Although poles cannot exist individually and always occur in pairs, it is convenient to utilize a unit magnetic pole, such a pole repels a similar pole. The magnetic field strength, H, is defined as the force per unit pole strength exerted by a magnetic monopole, P_2. The magnetic field strength H is the magnetic analog to the gravitational acceleration, g. It is given as (Burger *et al*., 2006):

$$H = \frac{F}{P_2} = \left(\frac{P_1}{\mu r^2}\right) \tag{3.2}$$

The SI unit of magnetic field strength H is the nanoTesla or nT

3.2.1 Magnetic Moment

The magnetic moment of a magnet is a quantity that determines the torque it will experience in an external magnetic field. Hence the magnetic moment is defined as a vector relating the aligning torque on the object from an externally applied magnetic field to the field vector itself. If a bar magnet is placed in a uniform magnetic field H, it will experience a pair of equal forces acting parallel to each other in opposite directions (a couple). The magnitude of the couple is

$$c = 2(ml)\underline{H}\sin\theta \quad (3.3)$$

where θ specifies the original orientation of the magnet in the field. The motion produced by the couple is dependent on the magnitude of H as well as the value of θ (no motion is produced if $\theta = 0$). The quantity (ml) called magnetic moment, M, affects the magnitude of the couple.

3.2.2 Intensity of Magnetization (I)

A magnetic material possesses a fundamental property (magnetic moment) per unit volume known as the intensity of magnetization I. The magnitude of I is defined as the magnetic moment M per unit volume.

$$I = \frac{M}{volume} \quad (3.4)$$

Therefore, since M = *ml*, Volume = l^3 and Area = l^2

$$I = \frac{M}{volume} = \frac{m}{area} \quad (3.5)$$

3.3 Total Magnetic Field B (Magnetic Induction)

The Earth's magnetic field is mostly caused by electric currents in the liquid outer core, which is composed of highly conductive molten iron. A magnetic field is generated by a feedback loop: current loops generate magnetic fields (Ampere's law); a changing magnetic field generates an electric field (Faraday's law); and the electric and magnetic fields exert a force on the charges that are flowing currents (the Lorentz force). These effects can be combined in an equation for the magnetic field and it is called the magnetic induction equation:

$$\frac{\partial \underline{H}}{\partial t} = \eta\nabla^2\underline{H} + \nabla\times(u\times\underline{H}) \quad (3.6)$$

where u is the velocity of the fluid, <u>H</u> is the magnetic H-field; and $\eta=1/\sigma\mu$ is the magnetic diffusivity with electrical conductivity (σ) and permeability (μ). This is a partial differential equation. The term $\partial H/\partial t$ is the time derivative of the field; ∇^2 is the Laplacian and $\nabla\times$ is the curl. The first term on the right hand side of the induction equation is a diffusion term. In a stationary fluid, the magnetic field declines and any concentrations of field spread out. If the Earth's dynamo shut off, the dipole part would disappear in a few tens of thousands of years (Ezema 2004). In the absence of an external magnetic field, individual magnetic domains within ferromagnetic material will be oriented in random directions and the net magnetic field will be zero. When placed in an external magnetic field, H_o such as the Earth's geomagnetic field, the magnetic domains will rotate toward the direction of the external field. Their orientation is no longer random and the material is said to be magnetized. The result is an induced net secondary field, H*s*. This secondary field is distinct from, but caused by, the (primary) inducing field. The situation is pictured in Figure 3.2

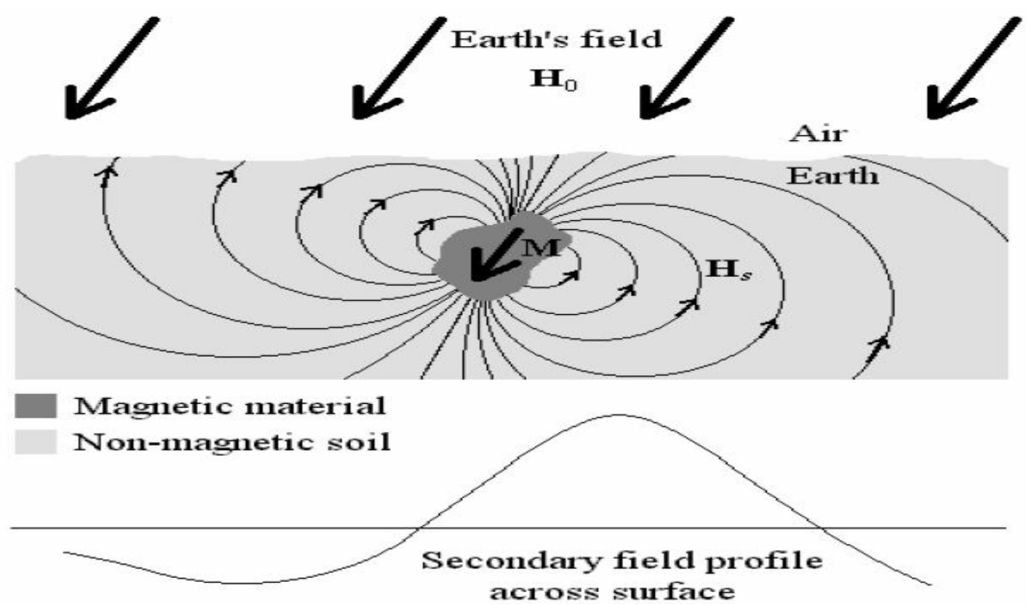

Figure 3.2: A schematic representation of magnetic induction of a magnetic body showing the primary inducing field, , the induced magnetization, M, and the associated secondary field, Hs (Lelièvre, 2003)

3.3.1 Magnetic Susceptibility k

Although the mechanisms by which induced magnetization can arise are rather complex, the field generated by these mechanisms can be quantified by a parameter known as the susceptibility, k. The determination of a material type through the knowledge of its susceptibility is an extremely difficult proposition, even more so than by determining a material type through knowledge of its density. Magnetic susceptibility is a dimensionless proportionality constant that indicates the degree of magnetization of a material in response to an applied magnetic field. For low magnetic field, magnetization M is proportional to the magnetizing field, that is;

$$M = k \underline{H} \tag{3.7}$$

where k is the constant of proportionality generally referred to as magnetic susceptibility, which is a fundamental rock parameter of magnetic prospecting. M is induced magnetization per unit volume and $\underline{H}$ is the field intensity. It is important to note some examples of the mineral materials and their susceptibility values as shown in Tables 3.1 and Histogram showing susceptibilities of different rock types is shown in Figure 3.3.

3.3.2 Causes of Magnetic Susceptibilities

Atomically, susceptibility of a material is due to:

1 Rotation of electrons in various shells around the nucleus

2 The spin of the electrons.

3 Number of electron in each shell.

Table 3.1: Magnetic Susceptibilities of Some Mineral (Telford *et al*., 1990).

ROCKS	**AVERAGE MAGNETIC SUSCEPTIBILITY (SI).**
Dolomite	0.00012
Lime Stone	0.00031
Sands Stone	0.00038
Shale	0.00063
Amphibolite	0.00075
Schist	0.00126
Quartzite	0.00440
Slate	0.00628
Granite	0.00281
Olivine – Diabase	0.02513
Diabase	0.05655
Porphyry	0.06283
Gabro	0.07540
Basalt	0.07540
Diorite	0.08797
Peridotite	0.16336
Acidic Igneous	0.00817
Harmatite	0.00691
Magnetite	6.28300
Calcite and Quartz	0.01000

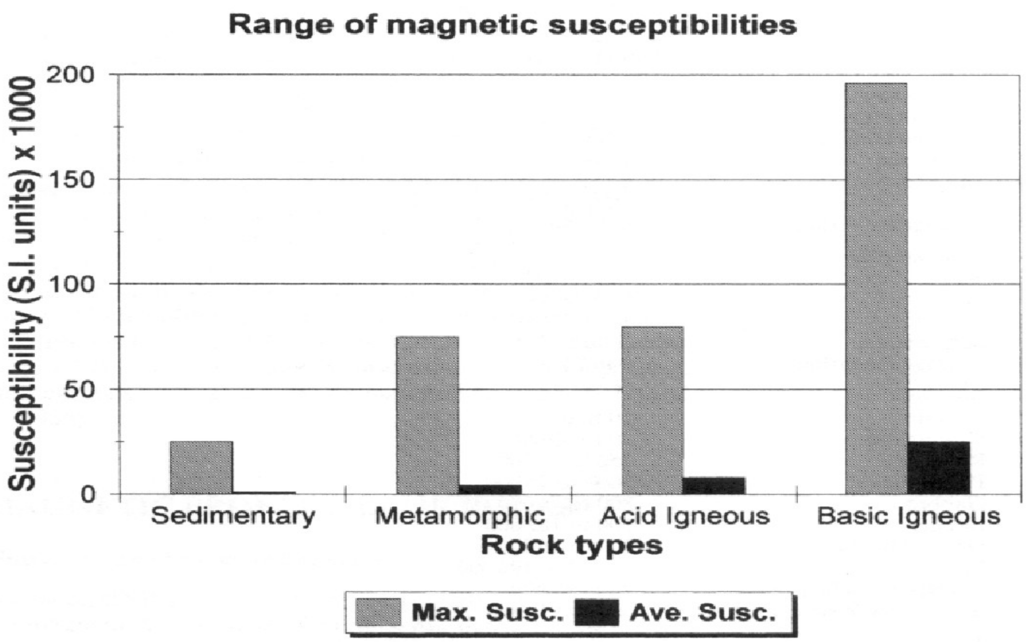

Figure 3.3: Histogram showing susceptibilities of different rock types (Telford *et al*., 1990)

3.4 Rock Magnetization

A rock may be regarded as a heterogeneous assemblage of minerals. The matrix minerals are mainly silicates or carbonates, which are diamagnetic in character. Interspersed in this matrix is a lesser quantity of secondary minerals (such as the clay minerals) that have paramagnetic properties. The bulk of the constituent minerals in a rock contribute to the magnetic susceptibility but are incapable of any contribution to the remanent magnetic properties, which are due to a dilute dispersion of ferromagnetic minerals (e.g. commonly less than 0.01% in a limestone). The variable concentrations of ferromagnetic and matrix minerals result in a wide range of susceptibilities in rocks (Fig. 3.3). The weak and variable concentration of ferromagnetic minerals plays a key role in determining the magnetic properties of the rock that are significant geologically and geophysically. The most important factors influencing rock magnetism are the type of ferromagnetic mineral, its grain size, and the manner in which it acquires a remanent magnetization. When the earth's magnetic field interacts with a magnetic mineral obtained in a rock, the rock becomes magnetized. This is called induced magnetism. The same thing occurs when an iron nail is placed near a bar magnet, the magnet's magnetic field will induce a magnetization in the iron nail. This induced field is often strong enough that you can pick up another smaller nail with the first nail. However, if the magnet is moved away from the nail, the induced magnetic field ceases.

3.4.1 Mechanisms for Induced Magnetization:

The nature of magnetization of material is in general complex, and governed by atomic properties. Hence there are three types of magnetic materials: paramagnetic, diamagnetic, and ferromagnetic.

Diamagnetism; This form of magnetism is a fundamental property of all materials and is caused by the alignment of magnetic moments associated with orbital electrons in the presence of an external magnetic field. For those elements with no unpaired electrons in their outer electron shells, this is the only form of magnetism observed. The susceptibilities of diamagnetic materials are relatively small and negative. Quartz and salt are two common diamagnetic earth materials.

Paramagnetism; This is a form of magnetism associated with elements that have an odd number of electrons in their outer electron shells. Paramagnetism is associated with the alignment of electron spin directions in the presence of an external magnetic field. It can only be observed at relatively low temperatures. The temperature above which paramagnetism is no longer observed is called the Curie temperature. The susceptibilities of paramagnetic substances are small and positive.

Ferromagnetism; This is a special case of paramagnetism in which there is an almost perfect alignment of electron spin directions within large portions of the material referred to as domains. Like paramagnetism, ferromagnetism is observed only at temperatures below the

Curie temperature. There are three varieties of ferromagnetism; Pure ferromagnetism, Antiferromagnetism and Ferromagnetism

Pure Ferromagnetism - The directions of electron spin alignment within each domain are almost all parallel to the direction of the external inducing field. Pure ferromagnetic substances have large (approaching one) positive susceptibilities. Ferrromagnetic minerals do not exist, but iron, cobalt, and nickel are examples of common ferromagnetic elements.

Antiferromagnetism - The directions of electron alignment within adjacent domains are opposite and the relative abundance of domains with each spin direction is approximately equal. The observed magnetic intensity for the material is almost zero. Thus, the susceptibilities of antiferromagnetic materials are almost zero. Hematite is an antiferromagnetic material.

Ferromagnetism - Like antiferromagnetic materials, adjacent domains produce magnetic intensities in opposite directions. The intensities associated with domains polarized in a direction opposite that of the external field, however, are weaker. The observed magnetic intensity for the entire material is in the direction of the inducing field but is much weaker than that observed for pure ferromagnetic materials. Thus, the susceptibilities for ferromagnetic materials are small and positive. The most important magnetic minerals are ferromagnetic and include magnetite, titanomagnetite, ilmenite, and pyrrhotite.

3.4.2 Remanent Magnetism

In many cases, the magnetization of rocks depends mainly on the present geomagnetic field and the magnetic mineral content. Residual magnetism (called Natural remanent magnetization, NRM) often contributes to the total magnetization, both in amplitude and direction. The effect is complicated because NRM depends on magnetic history of the rock. Natural remanent magnetization may be due to several causes. The principal ones are;

Thermoremanent Magnetization (TRM): This results when a magnetic material is cooled below the Curie point in the presence of an external field (usually the earth magnetic field). Its direction depends on the direction of the field at the same time and place where rock cooled. Remanence acquired in this is particularly stable. This is the main mechanism for the residual magnetization of igneous rock.

Detrital Magnetization (DRM) occurs during the slow settling of fine-grained particles in the presence of an external field. Varied clays exhibit this type of remanence.

Chemical remanent magnetization (CRM), takes place when magnetic grains increases in size or are changed from one form to another as a result of chemical action at moderate temperature, that is, below the curie point. This process may be significant in sedimentary and metamorphic rocks

Isothermic remanent magnetization (IRM) is the residual left following the removal of an external field. Lightning strikes produce IRM over very small areas.

Viscous remanent magnetization (VRM), is produced by long exposure to an external field; the buildup of remanence is a logarithmic function of time. VRM is probably more characteristic of fine-grained than coarse grained rocks. This remanence is quite stable (Telford *et al*., 1990)

3.5 The Earth Magnetic Field

The earth's magnetic field is like that of a large bar magnet placed at the centre of the earth or that due to a uniformly magnetized sphere (Fig. 3.1). To a first approximation, the geomagnetic field can be represented by a magnetic dipole situated at the centre of the earth. The magnetic field of the earth is a vector, that is, it has both magnitude and direction. Ninety percent of the earth's magnetic field looks like a magnetic field that would be generated from a dipolar magnetic source located at the center of the earth and aligned with the earth's rotational axis (Ezema 2004). The strength of the magnitude is about 60,000 nT. Figure 3.4 illustrates the difference between the earth's geographic, geomagnetic and magnetic poles and the equator.

The magnetic field of the earth can be classified into three separate components: Main field, External magnetic field and Crustal field.

The Main field is said to be the largest component of the magnetic field and is believed to be caused by electrical current in the earth's outer core. For exploration work, this field acts as the inducing magnetic field. It is not constant in time and varies relatively slowly. The External magnetic field is a relatively small portion of the observed magnetic field that is generated from magnetic sources external to the earth. It is partly cyclical and partly random. It is believed that this field is produced by interactions of earth's ionosphere with the solar wind; hence temporal variations associated with the external magnetic field are correlated to solar activity. Crustal field are basic targets in magnetic prospecting. It is otherwise a variation of the main field associated with the magnetism of crustal rocks. It contains magnetism caused by induction from the earth's main magnetic field and magnetism from remanent magnetization. The crustal field is usually but not always smaller than main field and it is relatively constant in time and place. Basically, it is caused by local magnetic anomalies in the near surface crust of the earth.

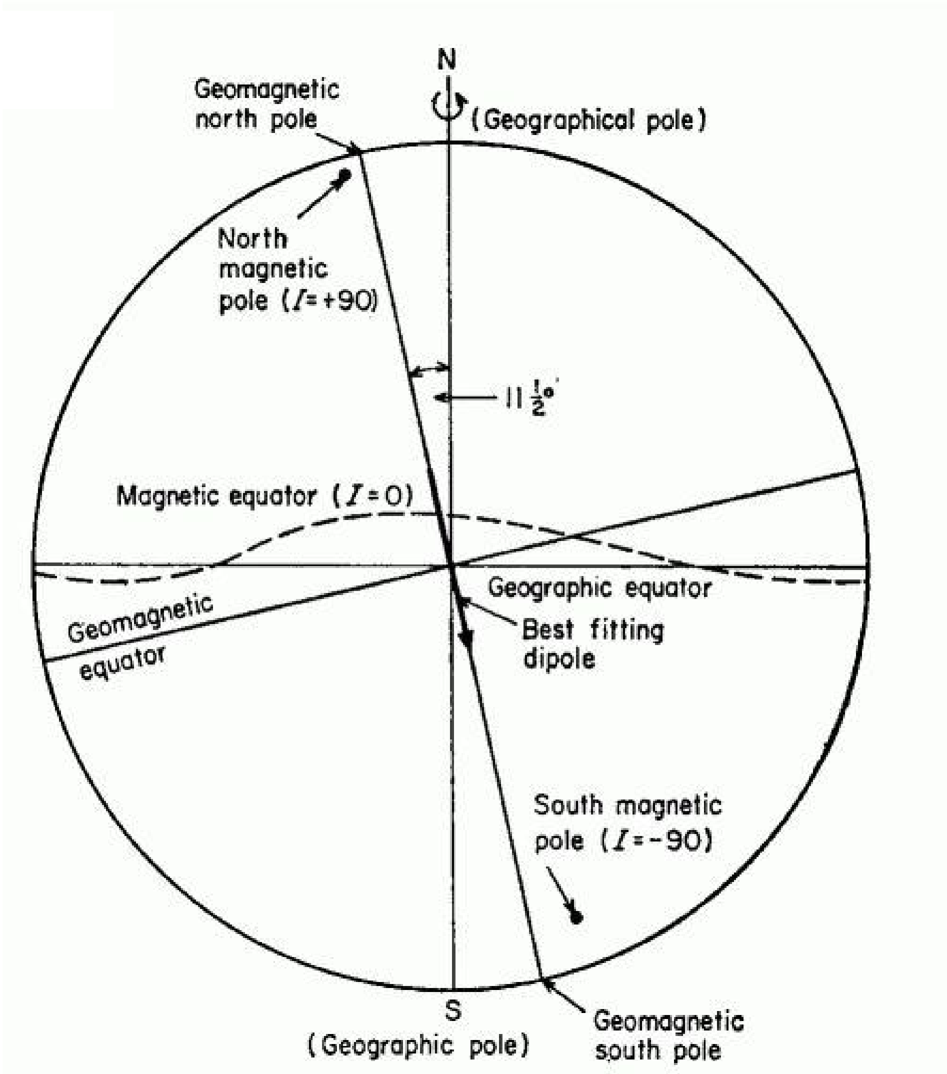

Figure 3.4: Illustrating the difference between the earth's geographic, geomagnetic, magnetic poles and the equator (McElhinny 1973)

On the surface of the earth, the 'South pole' of the equivalent bar magnet points to north geographical pole and the 'North pole' points to south geographical pole (Ezema 2004). As at present the best fitting dipole is aligned at 11.5^{o} to the earth's geographical north-south axis (spin axis). In Figure 3.4, geographic north and south poles, geomagnetic and geographic equators are shown. The points where the axis of the best-fitting dipole intersects the earth's surface are the geomagnetic North Pole at 79^{o}N, 71^{o}W and geomagnetic South Pole located at 79^{o}S, 109^{o}E respectively (Ezema 2004). Magnetic north and south poles are two points on the surface of the earth where the magnetic field is vertical and has no horizontal components. The magnetic north pole is at 76^{o}N, 101^{o}W while the south magnetic pole is at 66^{o}S, 141^{o}E. The geomagnetic equator is the equator of the best –fitting dipole axis while the magnetic equator is the line along which the magnetic field is horizontal and has no vertical component. The intensity of the dipole field is a function of the density of the 'flux lines' or magnetic induction B. The intensity is higher at the poles amounting to 60,000gammas which is twice its value at the equator of 30,000 gammas (Breiner, 1973)

3.5.1 Magnetic Elements and their Characteristics

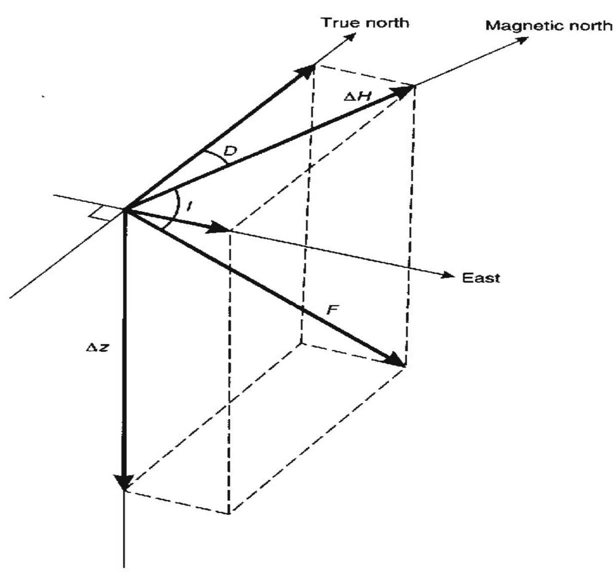

Figure 3.5: Elements of the earth's magnetic component (Lowrie, 1997)

The magnitude of the magnetic field, F, the inclination I and its declination D (the angle it makes with geographic north) all completely define the magnetic field. The elements as shown in Figure 3.5 can be grouped in pairs of three as (H, D, Z), (X, Y, Z) and (H, D, I), where H is the horizontal component, D is the declination angle (the angle between the vertical plane through the axis of the magnetic needle and the geographical north), Z is the vertical component, X is the north component, Y is the east component. I is the inclination angle or magnetic dip (angle by which a freely pivoted magnetic needle dips below the horizontal). It is positive when the north seeking pole of the needle points downward and negative if it points upwards. The Cartesian (X, Y, Z) and spherical polar F, D, I components are related as follows:

$$X = F\cos I\cos D, \qquad Z = F\sin I, \qquad D = \arctan\frac{Y}{X},$$

$$Y = F\cos I\sin D, \qquad \tan I = \frac{Z}{H}, \qquad I = \arctan\frac{Z}{\left(X^2+Y^2\right)^{1/2}},$$

$$H = F\cos I, \qquad F^2 = X^2+Y^2+Z^2,$$

The vertical plane through F and H is called the magnetic meridian. Lines of equal declination, inclination, horizontal intensity etc, when plotted on maps are usually referred to as isomap charts. They show the variation in the geomagnetic field over the earth's surface (Telford *et al.*, 1990)

3.6 The Geomagnetic Field

The dipolar nature of the geomagnetic field specifies the field's direction. The field is oriented vertically downward at the north magnetic pole. It is horizontal (and pointing north) at the magnetic equator and points vertically upward towards the south magnetic pole (Figure 3.4). The magnetic poles have been observed to have moved considerably over historical times and detectable movement occurs even from year to year (Ezema 2004). However, it is thought that on average over geological time, the dipole field which best fits the observed geomagnetic field has been coaxial with the geographic poles of rotation. However, at times the virtual magnetic poles may differ from the geographic poles by as much as 10 to 20 degrees. The definition of the main geomagnetic field at any point on the earth's surface as a vector quantity requires three scalar values (Figure 3.5), normally expressed either as three orthogonal components (vertical, horizontal-north and horizontal-east components) or the scalar magnitude of the total field vector and its orientation in dip and azimuth.

3.6.1 Temporal variation of the earth's magnetic field

These are time dependent variations and are resolved into secular changes, solar-diurnal changes, lunar diurnal changes and changes resulting from magnetic storms.

Secular variations: They are slow changes in the earth's field which take place progressively over centuries. They are usually noted in all magnetic elements at magnetic observatories everywhere in the world. The rate of change varies with time. Observations of Earth's magnetic field made over 400 years show a gradual change in position of the magnetic pole (Dobrin and Savit, 1988). They are also due to slow movement of eddy currents in earth's core.

Diurnal variations: These are daily changes in field due to changes in current charge particles in ionosphere. They are regularly recorded at magnetic observatories and are of more direct significance in magnetic prospecting. They are small but oscillate more rapidly in the earth's field with a periodicity of about a day and amplitude averaging about 25 gammas. The records of diurnal variations generally show two types of variations: the quiet day and the disturbed day. The quiet day variation is smooth, regular and low in amplitude. It can be separated into predictable components having both solar and lunar periodicities. The disturbed day is less regular and is associated with magnetic storms.

Magnetic storms: These are short term disturbances in magnetic field associated with sun spot activity and streams of charged particles from the sun. They can be up to 1000 nT in magnitude, and make magnetic surveying impossible. Magnetic survey must generally be discontinued during storms of any severity (Dobrin and Savit, 1988).

The Earth's total field: When a buried object has a magnetic field, such a field will be superimposed on that of the earth's magnetic field. The resultant field which will then be measured is a vector which will have both magnitude and direction. $T = T_o + \Delta T_a$, where T is the total field vector in the vicinity of the magnetic rocks, T_o is the earth's undisturbed field vector and ΔT_a is the anomalous magnetic field vector caused by the magnetized body. The measurement of the actual field by modern magnetic instruments is referred to as total field measurement. Generally, interpretation of total field varies in both magnitude and direction. It is more complex than those involving individual components, such as vertical measurement.

3.7 Aeromagnetic Data and Its Interpretation

Aeromagnetic data are made up of three data sets; the magnetic field measurement which is the primary data, base station data and the location recovery, generally in the form of station numbers transferred unto topography maps or sets of aerial photographs. Magnetic survey data are displayed as a set of profiles or a magnetic contour map. The procedure employed for processing magnetic data obtained from land is different from marine and airborne.

Usually data obtained from an aeromagnetic survey are often too large to be processed by hand. This gives rise to the use of modern computers for the processing of the data obtained. Interpretation is the extraction of geological information from a survey. The interpreter requires (a digital data files e.g. XYZ data) this vast quantity of numerical data to be presented in a format that can be appreciated by human perception. This involves going from digital data in a computer-storage media to maps and images that can be seen, examined and discussed. Interpretation usually has both qualitative and quantitative methods. Interpretation is therefore made to use the observation made in a survey to improve the description of the configuration of rocks in the ground that gives rise to the anomalies and to set limits to the depths, size, area extent, etc of each body causing an anomaly. The purpose of the data analysis and interpretation phase is to transform the data collected into credible evidence about the development of the intervention and its performance. It can be into two ways;

Qualitative Interpretation: It deals basically on maps interpretation on personal feelings or intuition or resulting from or pertaining to personal mindsets or experience, arising from perceptive mental conditions within the brain. It dominates the early stage of the map. It predicts anomalous bodies or structural style in subjective sense. Here, it is important to group similar responses into categories and identify common patterns that can help derive meaning from what may seem unrelated and diffuse responses. This is particularly important when trying to assess the outcomes of focus groups and interviews. Qualitative interpretation of the field data was first carried out by inspecting the total magnetic intensity (TMI) grid of the study area.

Quantitative Interpretation: It deals with how much deep the thing we are looking for inside the earth lies in an objective sense. It helps to measure the degree of change that has taken place in the study area and allows an assessment to be made about the consistency of data. Quantitative analysis involves the techniques by which researchers convert data to numerical forms and subject them to statistical analyses. It involves techniques that convert data into knowledge, i.e. Complex analysis and the analysis comes at the end of data collection. Numerical representation and manipulation of observations are done for the purpose of describing and explaining the phenomena that those observations reflect. The essence of quantitative interpretation is to obtain information about the magnetic source, its shape and size and detail about its susceptibility.

Magnetic data acquired on grids can be displayed and accessed from contour maps, area of sedimentary basin, igneous rocks, faults, fractures, etc. Computer contouring follows a different path from hand contouring. The z-values are required to be on a square grid during computer contouring which can be considered logically in three stages; gridding, contouring and plotting.

Gridding; Observational data are interpolated on to a grid because the XYZ data were collected over widely separated parallel lines which may have resulted in some points along the survey not sampled. It was important that the sampled data are represented by determining the values of points equally spaced far apart at the nodes of a grid. To produce the grids, ‘‘minimum curvature’’ method is used (Briggs, 1974). This method also called the random gridding method fits a minimum curvature surface (the smoothest possible surface that will fit given data values) to data points. The method was used because the data were sparsely sampled over wide area and continuous between data points. The RANGRID GX of the Oasis MontajTM software was used to achieve this. A grid size of 300m is used to avoid over or under sampling based on the sampling distance of the two data.

Contouring; gridded data are contoured to produce a plot file.

Plotting; the plot file is used to drive the physical plotting device. Interpretation is the extraction of geological information from a survey.

Polynomial Fitting; From the TMI grid, regional anomaly is separated from the residual anomaly by applying a second order polynomial which was fitted by least square method to the observed data. Different orders of polynomial are tried and it was found that the second order polynomial fitting was the best for our data as it reflected the geological information of the area.

Reduction to Pole; its operation was to restore the magnetic effect to appear as if it was collected at the North Pole. Upward Continuation is to enhance the data by 1-D Fast Fourier Transform (FFT). The fields were upward continued to the grid size of 300 m.

3.8 Magnetic Anomalies

Magnetic anomaly is a local variation in the Earth's magnetic field resulting from variations in the chemistry or magnetism of the rocks. Mapping of variation over an area is valuable in detecting structures obscured by overlying material. The magnetic variation in successive bands of ocean floor parallel with mid-ocean ridges is important evidence supporting the theory of seafloor spreading, central to plate tectonics. These layers are used for dating rocks.

3.9 Methodology

The following are the procedures employed in this research:

- Production of geographic and geology map of the study area.
- Merging of the two sheets data into one and Total Magnetic Intensity (TMI) of the study area was produced into maps which are in colour aggregate using WingLink, Oasis Montaj TM and Sufer 10 softwares.
- Application of Gridding, Filtering, Polynomial fitting (Regional and residual separation) and enhancement processes such as reduction to pole, derivatives and Upward and downward continuation to the TMI grid was achieved using WingLink software.
- TMI grid of the study area was later sectioned into eighteen cells, then smoothening of TMI, Fast Fourier Transform (FFT) complex, FFT Energy, FFT Frequency and Log of Energy (E) were deduced from each cell using Microsoft Excel.
- A plot of Log E against Frequency drawn for each cell and the slope of each cell was divided by 2π to determine the depth to magnetic source bodies (Spectral Analysis)

- Other depth evaluation methods such as Source Parameter Imaging (SPI) and forward and Inverse Modeling were also employed in quantitative interpretation.

3.10 Data Preparation and Processing:

Editing: This method involves removal of extraneous data after which the spikes in each data variable is removed from each line of survey.

Location: One of the difficulties encountered in airborne survey is the inability to know the particular location a given data was obtained. But the use of positioning systems such as GPS, VLF and so on, yields the absolute location a data was recorded on a digital tape and synchronize it with magnetic data. Hence the methods of determining and plotting the location depend on the positioning system used.

Data correction: Aeromagnetic data must be corrected for aircraft motion and temporal variation of the earth's magnetic field.

Time variation: They are those that are time dependent. Magnetic variations experienced during surveys are results of both geology and external influences on the earth's magnetic field.

Compensation: It is necessary to apply an active compensation system since the field of survey vehicle (aircraft) is a major source of error in an airborne survey.

IGRF removal: It is a mathematical representation of the earth's main magnetic field due to sources in the core. Once it is removed from the data, the remaining data becomes residual magnetic anomaly due solely to subsurface rocks.

Leveling: This is the distribution of erroneous data in such a way as to minimize their effects on localized anomalies. These errors are due to the minor flight elevation changes occurring along the flight lines by the aircraft.

Interpolation of regular grid: The data obtained becomes series of profile lines with a high data density along the lines and a low data density between the lines. In order to obtain contour maps, the data will then be reduced to a regular grid. This is known as interpolation.

Data display: The data may be displayed as residual contour maps, offset profiles and multi-parameter profiles.

3.11 Filtering Techniques

The initial stage of quantitative magnetic data interpretation involves the application of mathematical filters (reduction to pole, upward-downward continuation, first vertical derivative and first horizontal derivative) to the observed data. The specific goals of these filters vary, depending on the situation. The general purpose is to enhance anomalies of interest and to gain some basic information on source location or magnetization.

The upward projection (upward continuation) operation smoothen the anomalies obtained at the ground surface by projecting the surface mathematically upward above the original datum (Revees, 2005). By implementation of reduction to pole on both the amplitude and phase spectra of the original TMI grid, the shapes of the magnetic anomalies are simplified so that they appear like the positive anomalies located directly above the source expected for induced magnetized bodies at the magnetic pole where the angle of inclination is 90° and zero declination. A derivative (vertical and horizontal) helps to sharpen the edges of anomaly and enhances shallow features (Revees, 2005). This includes first and second vertical derivatives, and horizontal derivative. Computation of the first vertical derivative in an aeromagnetic survey is equivalent to observing the vertical gradient with a magnetic gradiometer with advantages of sharpening the edges of magnetic anomalies, enhancing shallow magnetic sources, suppressing deeper magnetic sources and giving a better resolution of closely spaced sources. Horizontal derivative was also calculated in the x and y directions.

3.12 Fourier Transform

The recent developments on Fourier transforms, for interpretation of gravity and magnetic anomalies have shown that the Discrete Fourier Transform on scattered data with 2-dimensional approach is given by (Billings *et al.*, 2002):

$$f_{mn} = \Delta u \Delta v \sum_{j=1}^{N/2} \sum_{k=1}^{M/2} F_{jk} \exp\left(-2\pi i\left(\frac{jn}{N}+\frac{km}{M}\right)\right) \qquad 3.8$$

where F_{jk} is the Fourier transform for the j^{-th} row and k^{-th} column in the frequency domain of the scattered data f_{mn} which represents the discrete data array of magnetic data, for the n^{th} row and the m^{th} column in the space domain, from N×M rectangular grid, with a spacing of Δx and Δy; i^2 = -1 is a complex number. Thus starting from F_{jk}, we deduce f_{mn} by inverse discrete Fourier transform, assuming grid spacing in the frequency domain Δu and Δv;

$$F_{jk} = \Delta x \Delta y \sum_{n=1}^{N} \sum_{m=1}^{M} f_{mn} \exp\left(-2\pi i\left(\frac{jn}{N}+\frac{km}{M}\right)\right) \qquad 3.9$$

As the data spacing Δx and Δy is approximately constant, an upper limit on frequencies resolved by the data can be estimated by the Nyquist relationship, U_{max}= 1/(2Δx) and V_{max}=1/(2Δy). Any higher frequencies that are present in the signal are aliased into the Nyquist limits. The Fourier transformations are used extensively in the processing of geophysical data (Billings *et al.*, 2002). They are required, among other things, to calculate the depth to basement from airborne magnetic surveys (Blakely,1995), to downward and upward continue magnetic surveys (Henderson and Zietz,1949), to calculate components of potential field in specified directions, in reduction to pole for magnetic survey (Ervin,1976). The algorithms of fast Fourier transform (FFT) were developed by Gentleman and Sande (1966) in order to reduce the maximum computing times. These algorithms are applied for the study of magnetic anomalies, by means of the processes of sampling. The transformed map in fact are obtained by controlled procedure of Fourier, who allows to realize at the same time, independently, two kinds of operations: on the one hand separation by frequential cut of part of the data, according to whether those require it or allow it; and on another hand, the vertical transformation, by derivation or prolongation of the data selected (Gerard and Griveau, 1972).

3.13 Spectral Analysis

Spectral analysis is a quantitative method, based on the properties of the energy spectrum of large and complex aeromagnetic data set. It uses the 2-D Fast Fourier Transform and transforms magnetic data from space domain to frequency domain. It makes it possible to consider the depth average of the bodies causing sources of anomalies. This method was used by several authors (Spector and Grant, 1970; Gerard & Debeglia, 1975; Bhattacharrya and Leu, 1975, 1977; Njandjock *et al.*, 2006) for the estimation of average depths of the magnetic or gravimetric source bodies. Pal *et al.* (1978) evoke that the transformation of Fourier of the gravimetric and magnetic anomalies of space to the frequential field, produces a method right for the estimate depth of the sources, when these sources are indicated by weak components of frequencies of the anomaly. The power spectrum function is transformed mathematically by technique of Fourier and the logarithm of the power contained in each frequency of the field that the sources create at a distance h, decreases linearly with increasing frequency within discrete segments of the spectrum (Tadjou *et al.*, 2009). Thus, the depth h of the roof of the body can be estimated by the formula (Tadjou *et al.*, 2009):

$$h = \frac{\Delta \log(E)}{2\pi\Delta(f)} \qquad 3.10$$

From Eqn (3.10), it follows that; $M = \frac{\Delta \log(E)}{\Delta(f)}$. Hence,

$$h = \frac{M}{2\pi} \qquad \text{and} \qquad 2\pi h = M \tag{3.11}$$

where $E(f) = e^{-2hf} = |F(f)|^2$ is the energy spectrum (the square of the Fourier amplitude spectrum) and ΔLog (E) is the variation of the logarithm of the power spectrum in the interval of frequency Δ(f). The energy spectrum generally has two sources. The deeper source is manifested in the smaller wavenumber end of the spectrum, while the shallower ensemble manifests itself in the larger wavenumber end. The tail of the spectrum is a consequence of high wavenumber noise (Tadjou *et al.*, 2009). The graph of Log E against Frequency is drawn for the eighteen cells.

3.14 Source Parameter Imaging (SPI)

This method calculates source parameters for gridded magnetic data. The method assumes either a 2D slopping contact or a 2D dipping thin-sheet model and is based on the complex analytic signal. Thurston *et al*. (2002) referred to source parameter imaging as the wave number method which is a profile or grid-based method for estimating magnetic source depths and for some source geometries, the dip and susceptibility contrast. The basics are that for vertical contact, the peaks of the local wave number define the inverse of depth. In otherwords, the expression for SPI depth is (Thurston and Smith, 1997);

$$\text{Depth} = \frac{1}{K_{\max}} = \frac{1}{\left(\sqrt{\left(\partial Tilt/\partial x\right)^2 + \left(\partial Tilt/\partial y\right)^2}\right)_{\max}} \tag{3.12}$$

where Tilt is

$$Tilt = \arctan\left(\frac{\partial T/\partial z}{\left(\sqrt{\left(\partial T/\partial x\right)^2 + \left(\partial T/\partial y\right)^2}\right)}\right) \qquad 3.13$$

$$Tilt = \arctan\frac{\partial T/\partial z}{HGRAD} \qquad 3.14$$

where HGRAD = horizontal gardient, T= total magnetic intensity (TMI), $\partial T/\partial x$, $\partial T/\partial y$, $\partial T/\partial z$ are the derivatives of TMI with respect to x, y and z representing the horizontal and vertical components of earth's field. SPI algorithm of Oasis Montaj^{TM} is employed to locate and estimate the depths of anomalous sources and depths to basement by calculating the horizontal grids, applying a cut off depth consistent with geology of area and then obtaining the SPI grid.

3.15 Forward and Inverse Modelling

Forward modeling involves the comparison of the calculated field of a hypothetical source with that of the observed data; the model is adjusted in order to improve the fit for a subsequent comparison. Inverse modeling involved direct determination of some parameters of the source from the measured data. The software used for the forward and inverse modeling of the anomalies over the study area was Potent software. Potent in essence is software or a program for modeling the magnetic and gravitational effects of subsurface and also an extension in the Oasis Montaj^{TM} software. Main concepts in Potent include; Observation, Model, Calculation, Visualization and Inversion. Interpretation of magnetic field data using Potent starts with the observation of the image of the observed data (Obiora *et al.,* 2016). The primary function of the program is to bring these concepts together in a coherent and intuitive way.

Observation: potent interprets magnetic field data by observing the image of the observed data which shows contours of the observed total magnetic intensity (TMI) of the study area. The observed field often has a regional field superimposed on anomalies of interest. Such a background field might arise from deep sources that produce long wavelength anomalies that are of no interest in the cause of the interpretation. This background field is known as the regional field. This long wavelength regional field needs to be removed from the observed field to give the residual field required for interpretation.

Model: The main task of the interpreter is to create a model that is geophysically plausible and consistent with the observed field values. The following geometrical bodies can be created: sphere, rectangular prism, dyke, slab, ellipsoid, etc. By trial and error approach, these bodies were attempted in modeling the observed data in order to obtain the best fit model. In trying to model the observed data, potent assigns the body default parameters (shape, position and physical properties).The body created was then modeled by varying any or all the parameters of the body.

Calculation: the model is consistent with the observed physical values if its calculated field matches the observed values to some degree of precision. This was done by calculating the total magnetic field intensity due to the model and comparing it with the observed field. Potent automatically calculated the field due to the model in response to the changes made to the model.

Visualization: This part is inherent because the interpreter subjectively asses the match between the observed and calculated physical values by visualizing them.

Inversion: Inversion method is a mathematical process that automatically adjusts model parameters so as to improve the fit between the calculated field and the observed field. It is customary to begin inversion with a reasonable starting model that is both geologically sensible and has a calculated field that is similar to the observed field. The inversion procedure was performed using a single component data (TMI) for multiple bodies. The data points in the sample of observed data provided the geographic coordinates (X, Y, and Z) at which potent calculated the field due to the model. Secondly they provided the observed field values, F, against which the calculated field values were compared. The inversion algorithm then attempted to minimize the root-mean-square values (RMS) difference between the observed and calculated field values. The RMS value was then displayed at the end of the inversion, as the fit between the observed and calculated field continue to improve, the RMS value decreases until a reasonable inversion result is achieved.

3.16 Source of Data

Nsukka (sheet 287) and Udi (sheet 301) data were obtained from the Nigerian Geological Survey Agency (NGSA). The data, covering one hour (One degree) by thirty minutes (Half-degree) sheet and in scale of 1:100,000 were acquired at a flight altitude of 80 m, along NE-SW flight lines that were spaced at 500 m. It was recorded in digitized form (X, Y, Z text file) after removing the geomagnetic gradient from the raw data using International Geomagnetic Reference Field (IGRF), 2009, with intensity of 33095 nT (nanoTesla), angles of inclination and declination of -13.2785° and -1.449°, respectively. The X and Y represent the longitude and latitude of Nsukka and Udi in meters respectively, while the Z represents the magnetic field intensity measured in nanoTesla. Noise (Random noise) was removed by upward continuation of the aeromagnetic anomaly field to a height of 125 m before producing the upward continued aeromagnetic anomaly map of the sheet in coloured.

CHAPTER FOUR

RESULTS AND DISCUSSION

4.1 Qualitative Map Results

The total magnetic intensity (TMI) map of the study area was produced into maps in colour aggregate (Fig 4.1). The total magnetic intensity varies from -110 nT to 140 nT. The area is marked by the high (red colour) and low (green, blue and yellow colours) magnetic signatures. The variation in magnetic intensity could be as a result of degree of strike, variation in depth, difference in magnetic susceptibility, difference in lithology, dip and plunge. In TMI curve (Fig 4.1) we can observe obvious contour truncation, linear alignment of circular bodies and colour matching, which gives room for the presence of faults (the standard recognized fault signature is a steep gradient, whether it is on a gravity, magnetic, or a seismic time map), synclines (a syncline produces a minimum closure on most geophysical maps), anticlines (a simple folded symmetrical anticlines produces a symmetrical positive magnetic anomaly), dipping beds (a dipping bed produces an anomaly similar to that of a fault, but the main difference is that as the bed nears the surface, the gradient of the anomaly becomes steeper and the magnitude of the anomaly tends to be greater), dyke and intrusive.

Upward and downward continuation are processes by which potential field data from one datum surface are mathematically projected (upward or downward) to level surfaces above or below the original datum. In projecting to a higher plane, we are effectively smoothing. That is, suppressing the effect of local (residual) anomalies and enhancing regional effects. On the other hand, in projecting downward, the regional effects are suppressed while the residual effects are enhanced. Figure 4.2 shows the Upward and Downward Continuation map of the study area.

Vertical and horizontal derivatives analyses are useful in mineral prospecting to enhance small scale features near the surface. First vertical and horizontal derivatives were obtained from the data. Figures 4.3 and 4.4 show the First Vertical Derivative and First Horinzontal Derivative maps of the study area. First vertical derivative (FVD) enhanced shallow sources by suppressing deeper ones and gave a better resolution to closely spaced sources.

Reduction to pole entails removing the dependence of magnetic data on the magnetic inclination, which is converting data which were recorded in the inclined Earth's magnetic field to what they would have been if the magnetic field had been vertical or as if it were at pole. This method has simplified the interpretation because for sub-vertical prisms or sub-vertical contacts (including faults), it transforms their asymmetric responses to simpler symmetric and anti-symmetric forms. The symmetric "highs" are directly centered on the body, while the maximum gradient of the anti-symmetric dipolar anomalies coincides exactly with the body edges. Reduction to pole was performed on the digitized aeromagnetic data of the study area and it is seen in Figure 4.5.

The regional field was removed from the total magnetic intensity map to obtain the residual map with a first order polynomial fitting using WinGlink Software. Figures 4.6 and 4.7 show the regional and residual maps of the area respectively. The TMI map was subdivided into 18 spectral blocks allowing spectral probe of 18.33 km by 18.33 km area. The regional map of the study area varies from -10 nT to 85 nT while the residual map varies from -150 nT to 120 nT.

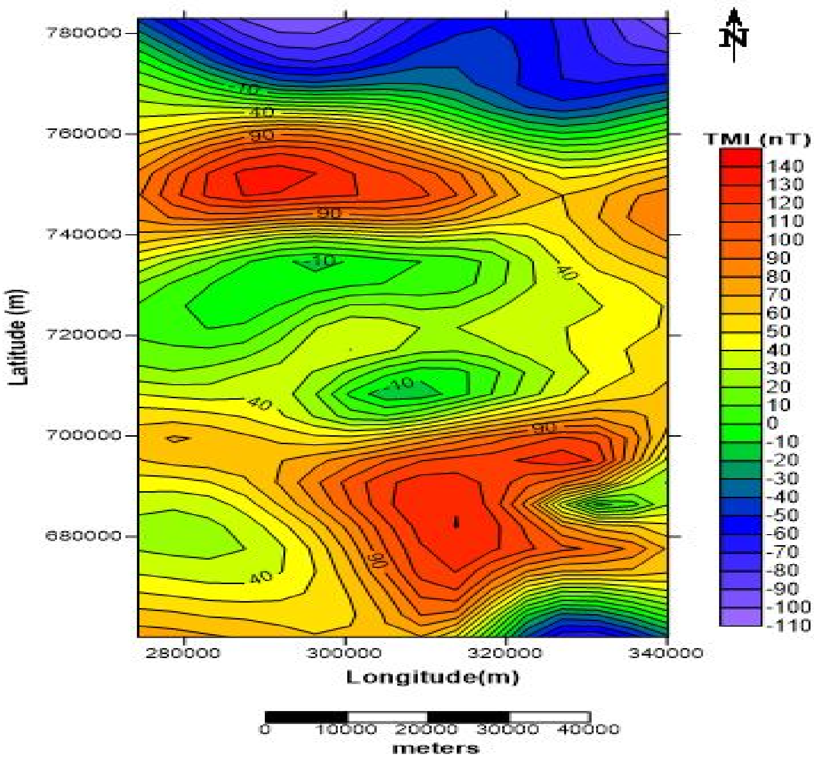

Figure 4.1: TMI Map of the Study Area

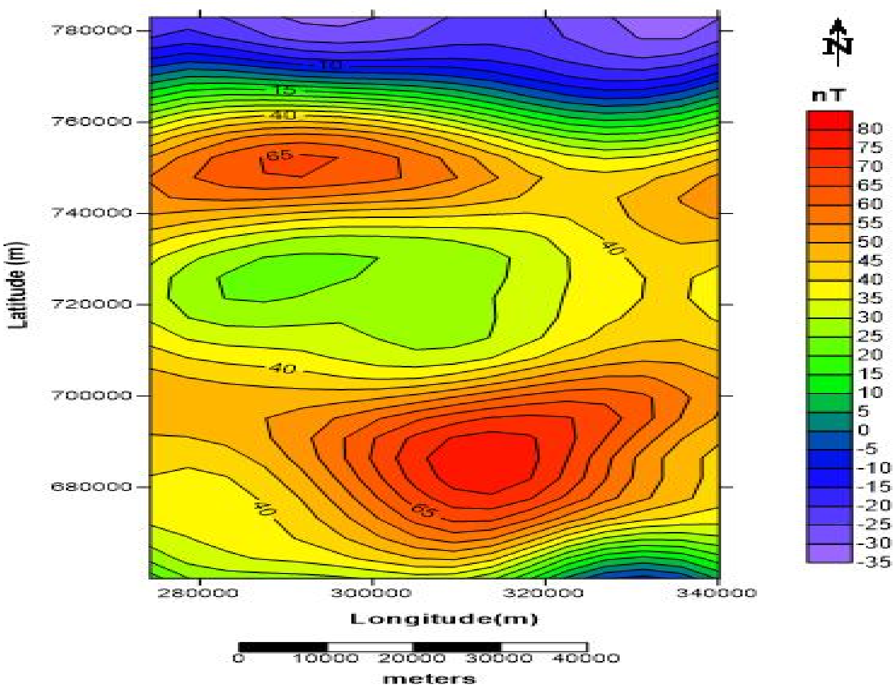

Figure 4.2: Upward and Downward Continuation Map of the Study Area

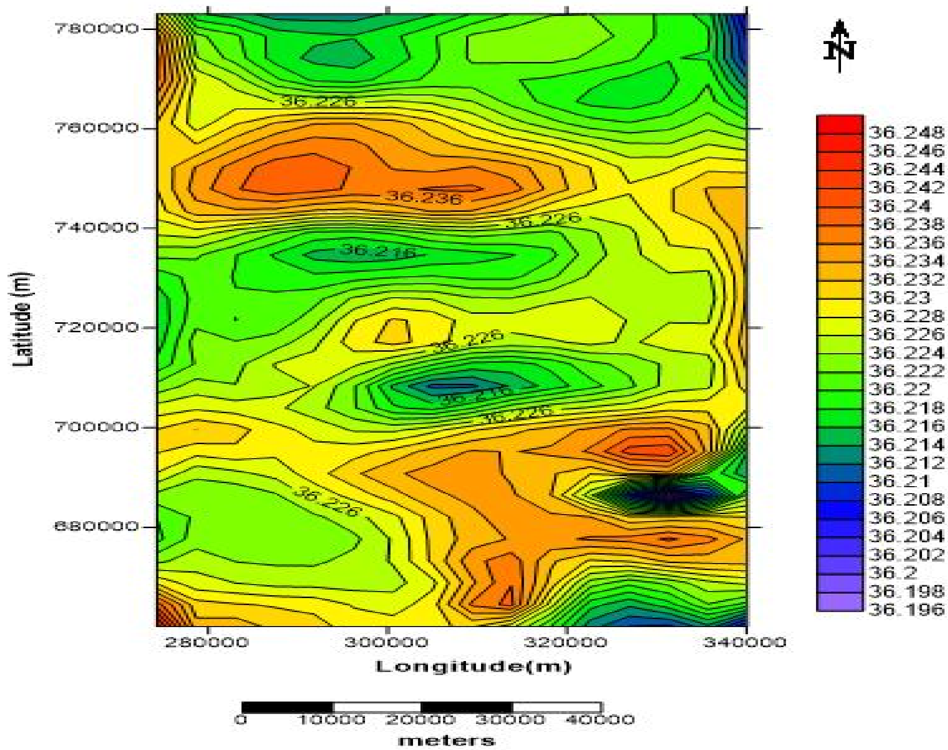

Figure 4.3: First Vertical Derivative Map of the Study Area

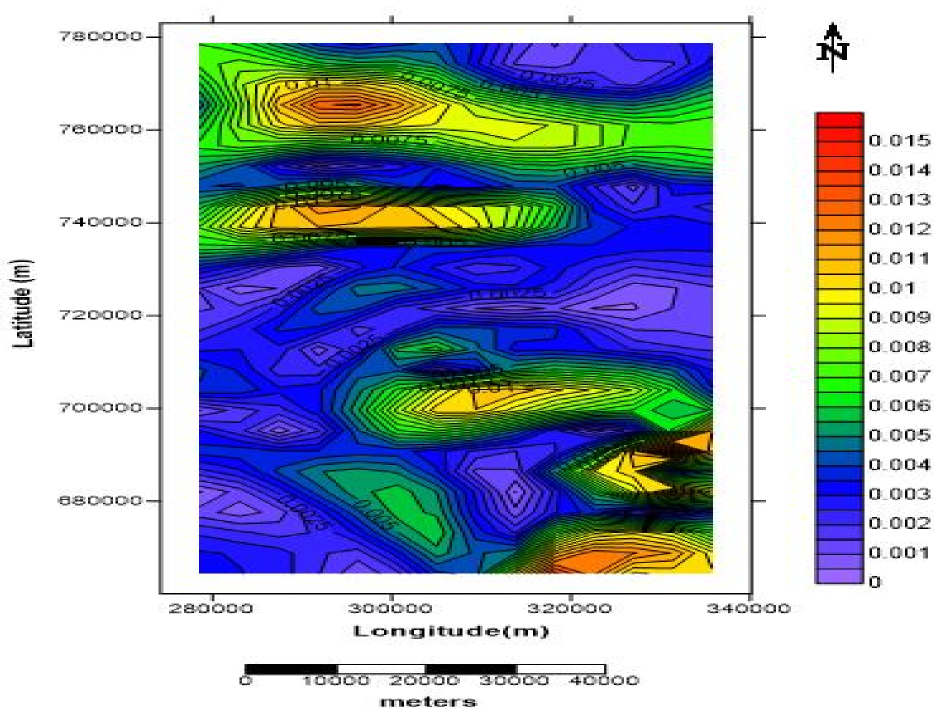

Figure 4.4: First Horizontal Derivative Map of the Study Area

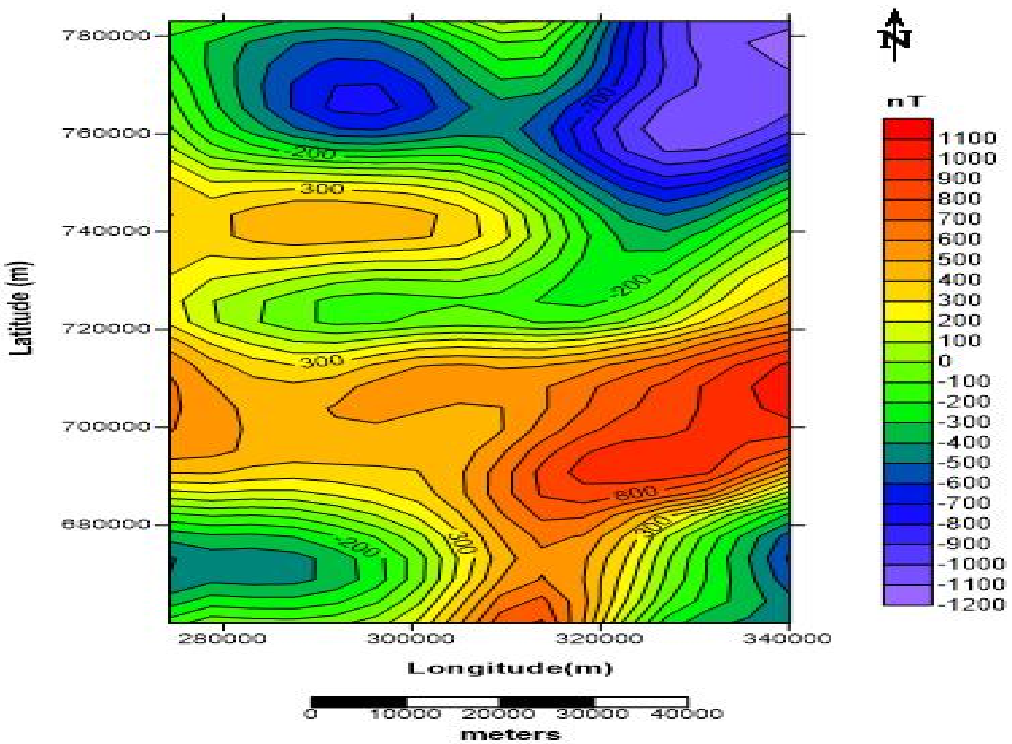

Figure 4.5: Map Showing the Reduction to Pole of the Data

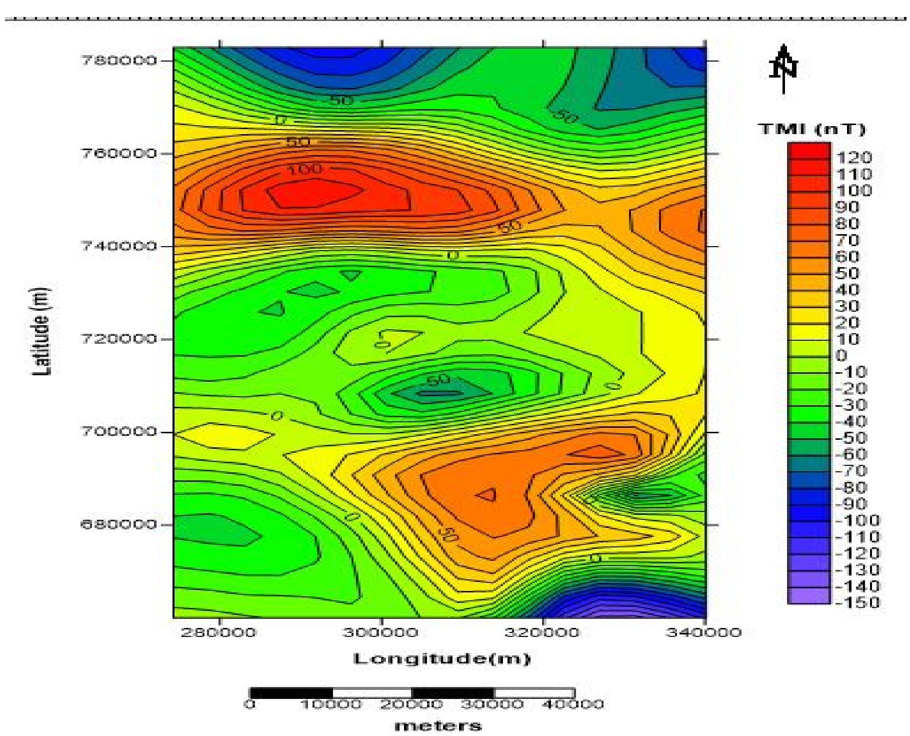

Figure 4.6: Residual Map of the Study Area

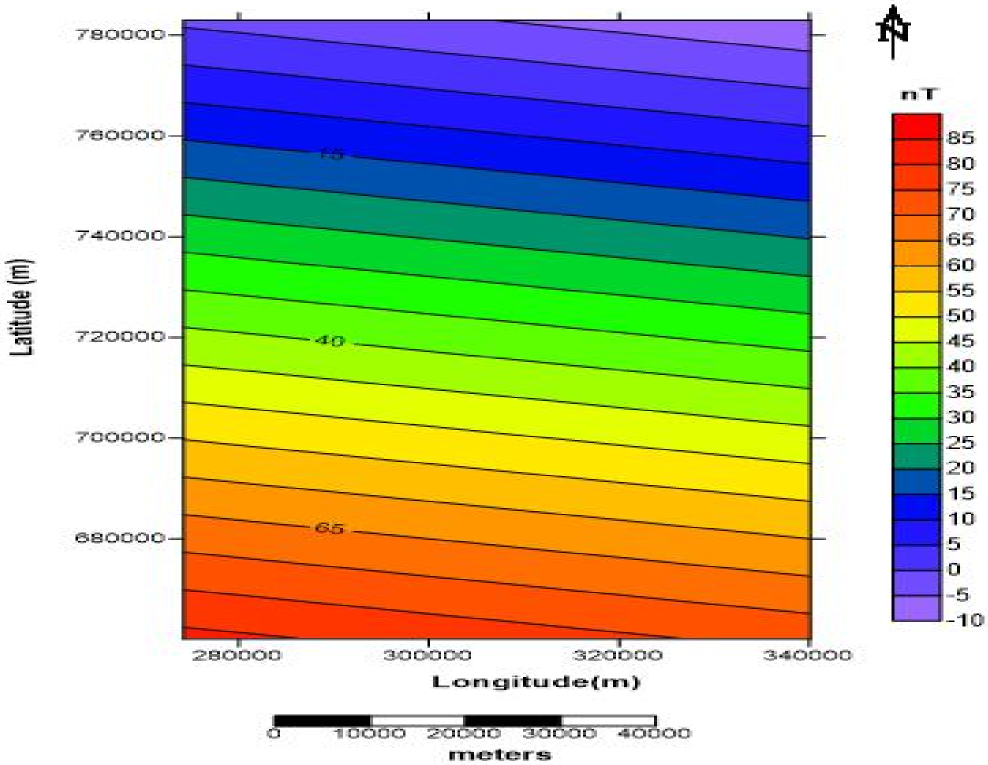

Figure 4.7: The Regional Map of the Study Area

4.2 Quantitative Interpretation of Maps

This involves making numerical estimates of the depth and dimensions of the sources of anomalies and this often takes the form of modelling of sources which could in theory replicate the anomalies recorded in the survey. It is also seen as other reliable methods to affirm what was predicted. Some quantitative methods of aeromagnetic data interpretation that were used include; spectral analysis, source parameter imaging (SPI), forward and inverse methods.

4.2.1.1 Spectral Analysis (Interpretation and Results): Here, the study area was divided into eighteen cells or spectral blocks for the purpose of easier handling of the large surface area involved (Fig 4.8)

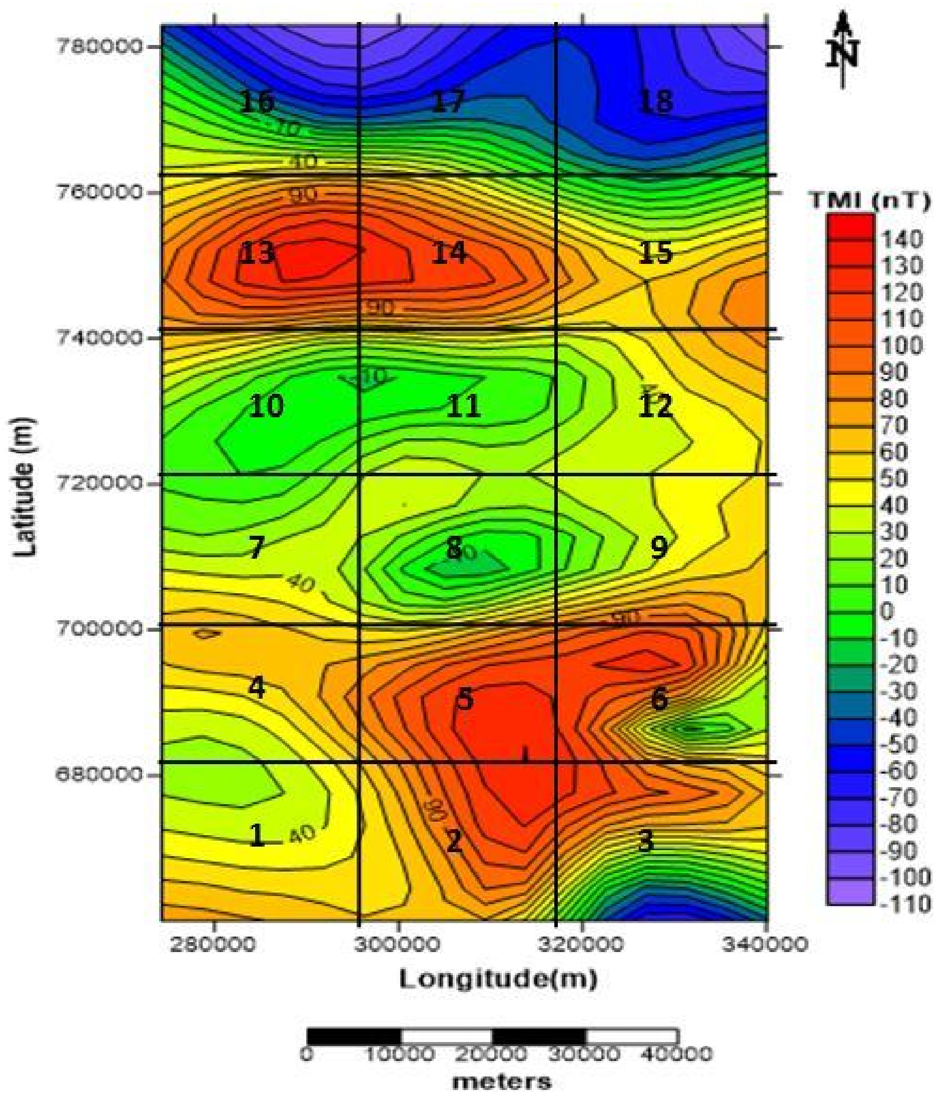

Figure 4.8: Map Showing Spectral Cell Division

4.2.1.1 Plots of Log of Energy and the frequency: Fig. 4.9 shows the graph of Log E against Frequency for the eighteen spectral blocks or cells. For each cell, two linear segments can be identified which implies that there are two magnetic source layers in the study area; the deep and shallow magnetic sources of the gradients are represented by arrow head and line respectively.

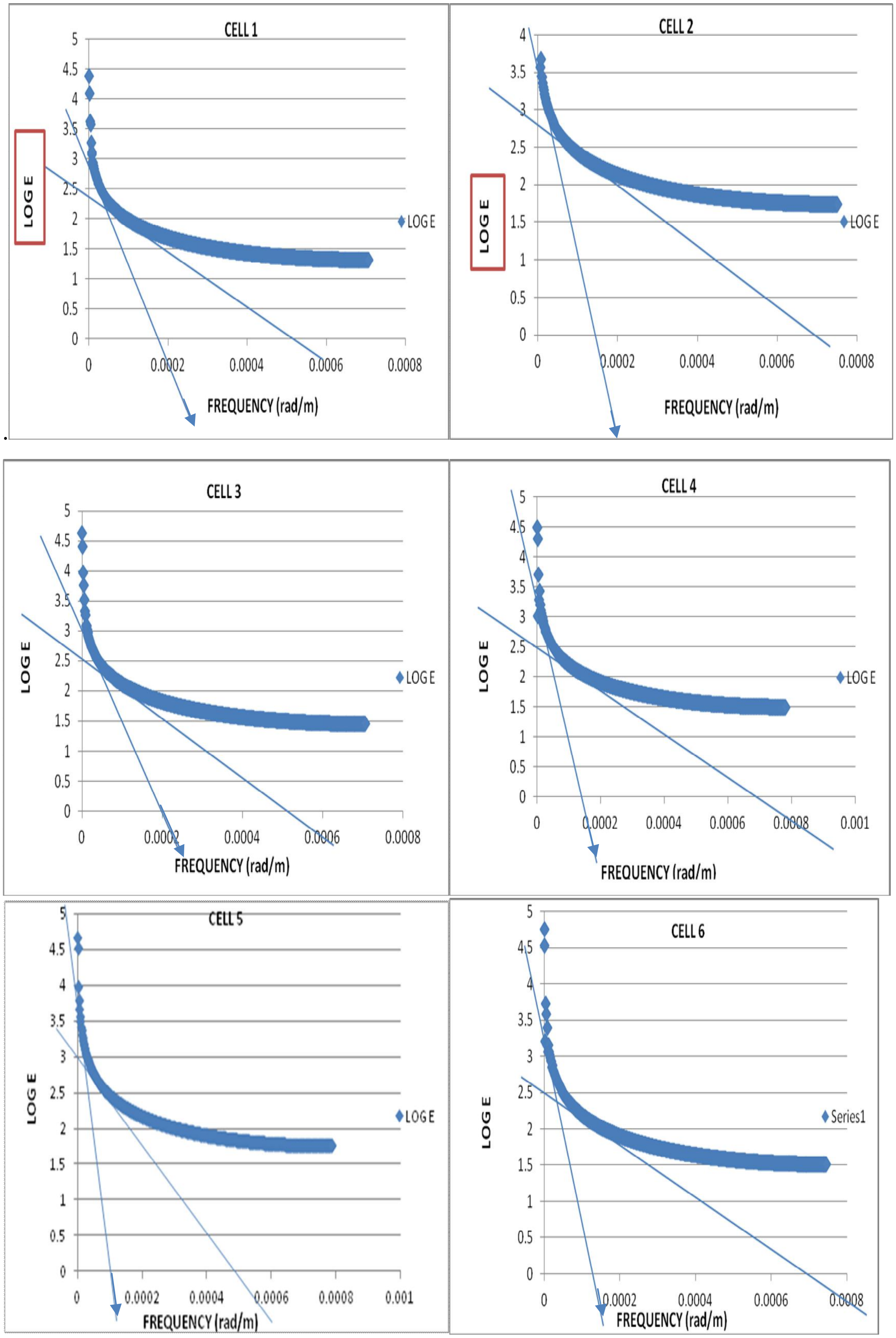

Figure 4.9: Spectral plots of Log E against Frequency (rad/m) of cells 1 – 6

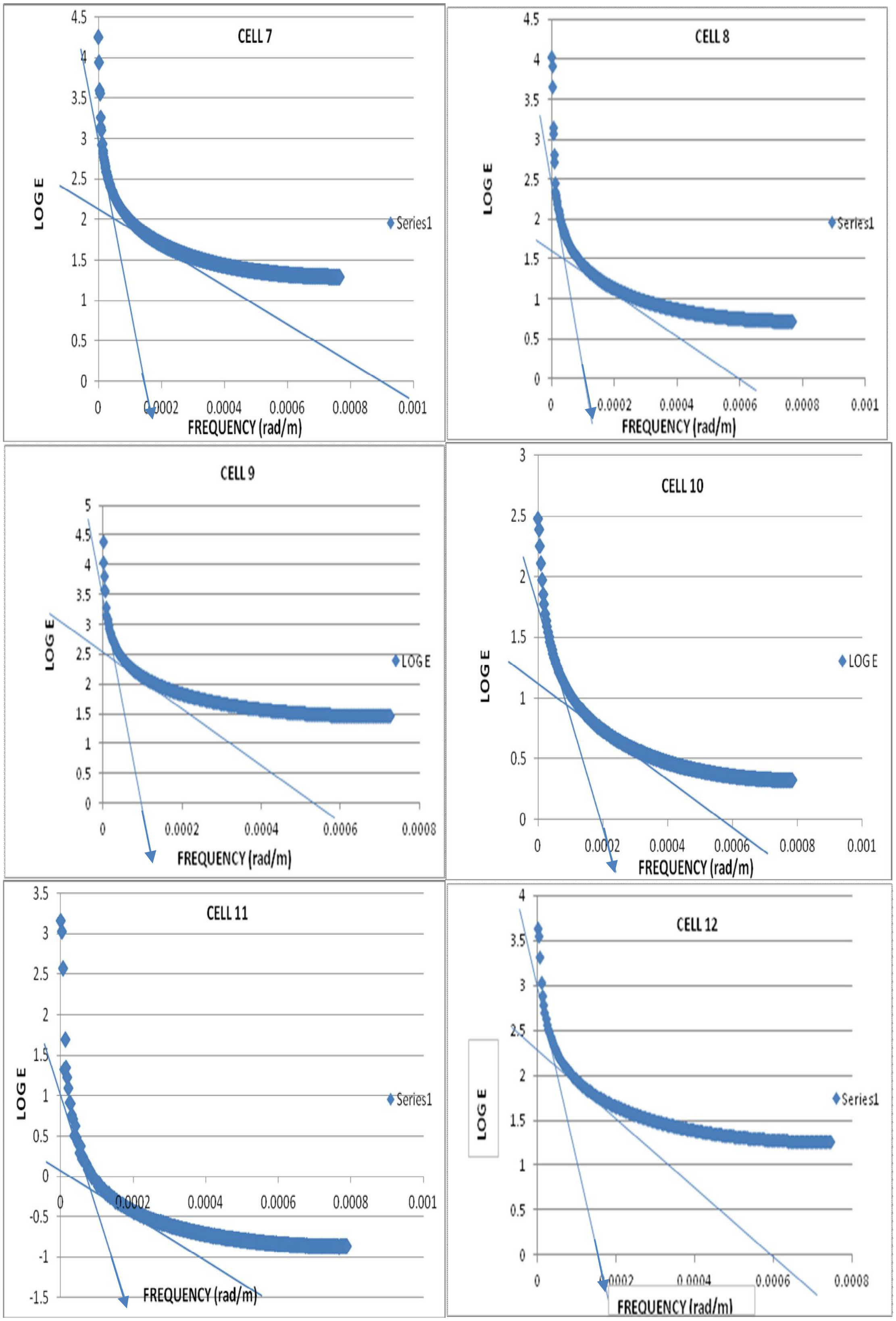

Figure 4.10: Spectral plots of Log E against Frequency (rad/m) of cells 7 – 12

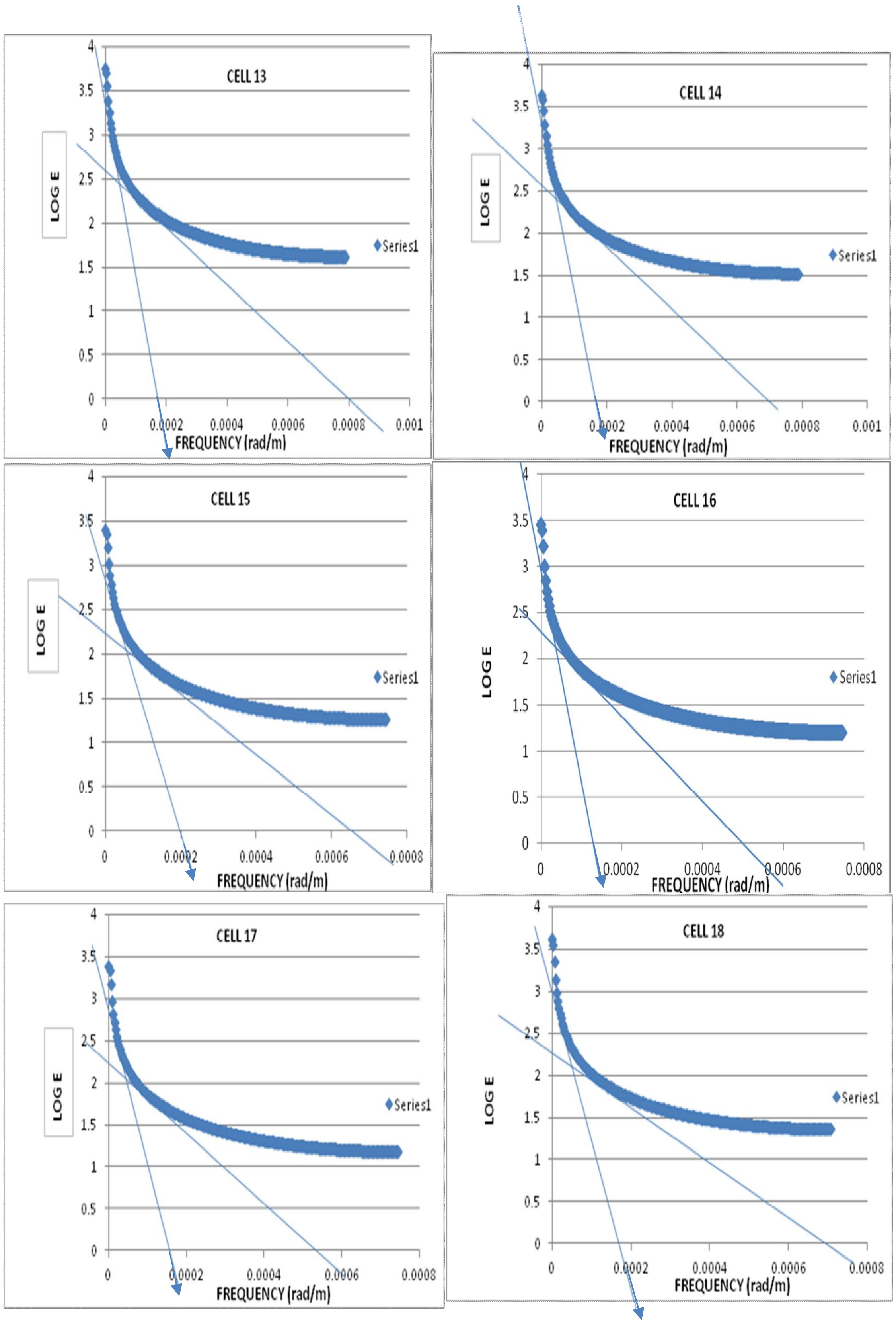

Figure 4.11: Spectral plots of Log E against Frequency (rad/m) of cells 13 – 18

4.2.1.2 Estimation of Depth to Magnetic Sources

Using the plots shown in Figures 4.9 - 4.11, equation 3.10 was used to compute the depths of shallow (Table 4.2) and deeper magnetic sources (Table 4.1) and the summarized result is shown in Table 4.3.

Table 4.1: Summary of the Log E/Frequency Graph for Deeper Slope

CELL NO:	LOG E	FREQ (m)	SLOPE $\Delta LogE/\Delta Freq$	DEPTH DEEPER (m) (Slope/2π)
1	2.9	0.00018	16111.111	2564.162972
2	3.5	0.00015	23333.333	3713.615338
3	3	0.0002	15000	2387.324146
4	3.3333	0.00015	22222	3536.741145
5	3.7	0.0001	37000	5888.732894
6	3.25	0.00014	23214.286	3694.668321
7	3	0.00015	20000	3183.098861
8	2.5	0.0001	25000	3978.873577
9	3.5	0.0001	35000	5570.423007
10	1.75	0.00019	9210.5263	1465.900791
11	1	0.00008	12500	1989.436788
12	3	0.00016	18750	2984.155183
13	3.375	0.00017	19852.941	3159.693723
14	3.25	0.00017	19117.647	3042.668029
15	2.8	0.0002	14000	2228.169203
16	3	0.00012	25000	3978.873577
17	2.85	0.00017	16764.706	2668.18581
18	3	0.00018	16666.667	2652.582385
Average				3260.405875

Table 4.2: Summary of the Log E/Frequency Graph for Shallow Slope

CELL NO:	LOG E	FREQ (m)	SLOPE $\Delta LogE/\Delta Freq$	SHALLOW DEPTH (m) (Slope/2π)
1	2.3333	0.00052	4487.115	714.1465936
2	2.75	0.0007	3928.571	625.2515621
3	2.5	0.0005	5000	795.7747154
4	2.5	0.0007	3571.429	568.410511
5	3	0.0005	6000	954.9296584
6	2.5	0.0007	3571.429	568.410511
7	2.125	0.0009	2361.111	375.7825045
8	1.625	0.0006	2708.333	431.0446375
9	2.6667	0.00054	4938.333	785.9601605
10	1.125	0.00057	1973.684	314.1215982
11	0.16667	0.000025	6666.8	1061.054174
12	2.3	0.0006	3833.333	610.0939484
13	2.625	0.0008	3281.25	522.227157
14	2.625	0.0007	3750	596.8310365
15	2.25	0.00065	3461.538	550.9209568
16	2.3	0.0005	4600	732.1127381
17	2.25	0.00054	4166.667	663.1455961
18	2.25	0.0007	3214.286	511.5694599
Average				632.3215288

Table 4.3: Summary of Spectral Analysis Result

Cell No.	Median Long. (m)	Median Lat.(m)	Deeper depth(m)	Shallow depth (m)
1	287650	673450	2564.162972	714.1465936
2	306150	673450	3713.615338	625.2515621
3	324650	673450	2387.324146	795.7747154
4	287650	691450	3536.741145	568.410511
5	306150	691950	5888.732894	954.9296584
6	324650	691950	3694.668321	568.410511
7	288275.2	710450	3183.098861	375.7825045
8	306275.2	710450	3978.873577	431.0446375
9	324650	710450	5570.423007	785.9601605
10	288400.4	728718.1	1465.900791	314.1215982
11	306900.4	729218	1989.436788	1061.054174
12	328400.4	728718.1	2984.155183	610.0939484
13	288400.4	746718.1	3159.693723	522.227157
14	306400.4	746718.1	3042.668029	596.8310365
15	324900.4	746718.1	2228.169203	550.9209568
16	288400.4	765218.1	3978.873577	732.1127381
17	306400.4	765218.1	2668.18581	663.1455961
18	324900.4	765218.1	2652.582385	511.5694599
Average			3260.405875	632.3215288

4.2.1.2.1 Magnetic Basement Depth Map: Using the computed spectral values (Table 4.3), the magnetic basement depth map was plotted and contoured using surfer 10 software. The depth of the shallower magnetic sources (Table 4.2) varies from 314 m to 1061 m with an average depth of 632.3 m, whereas the depths of the deeper magnetic sources vary from 1465.9 to 5888.7 m with an average value of 3260.4 m. Figures 4.12(a,b) show respectively, the 2D and 3D contour maps of the shallow magnetic source depth while Figure 4.13(a,b) show that of the deeper depth of magnetic basement.

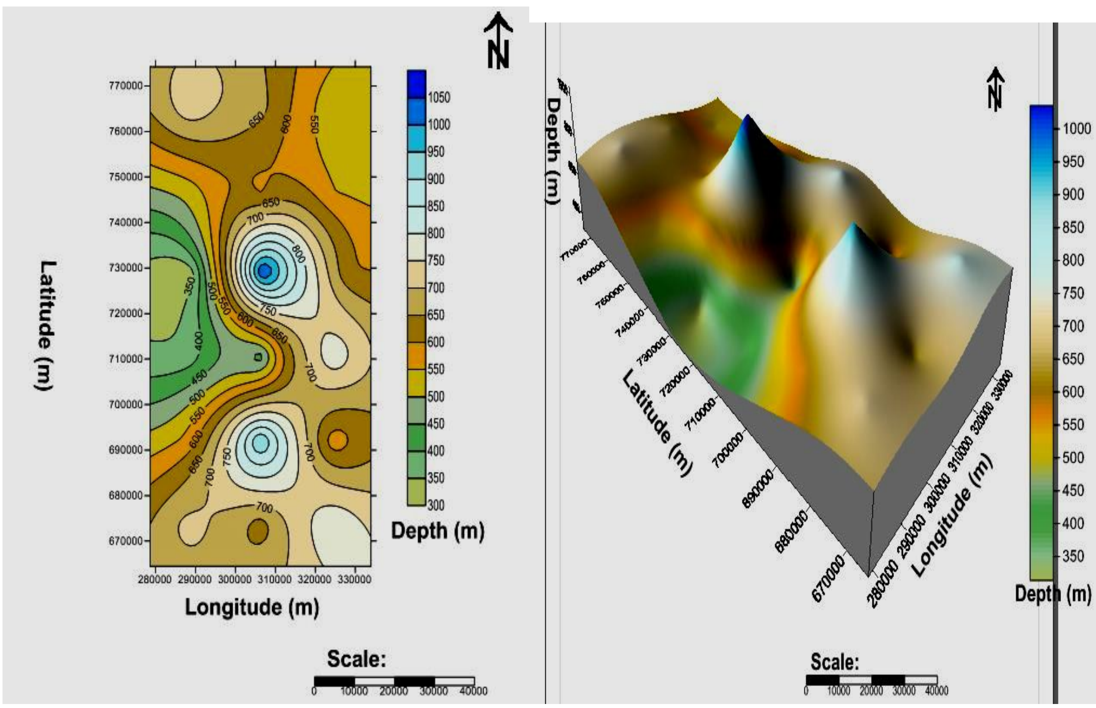

Figure 4.12: (a) Map of 2D Shallow Depth of Basement (b) Map of 3D Shallow Depth of Basement

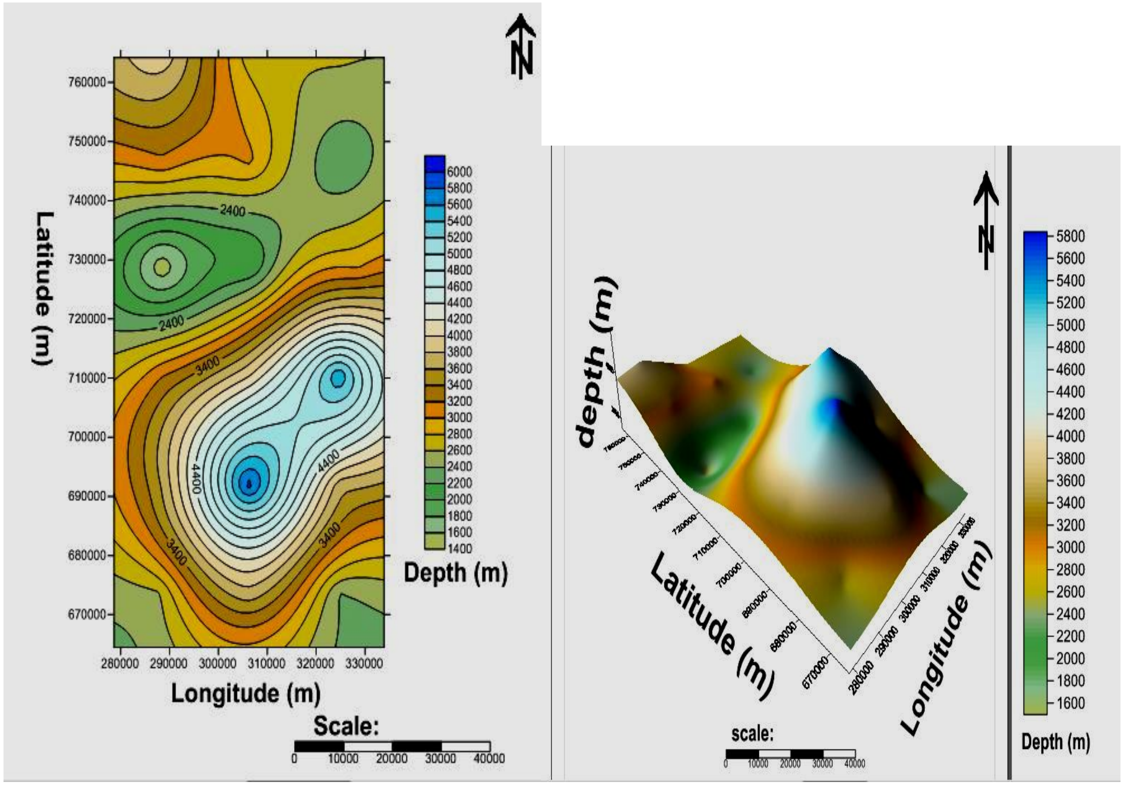

Fig 4.13: (a) Showing 2D Deeper Depth of Basement (b) Showing the 3D Deeper Depth of Basement

4.2.2 Source Parameter Imaging (SPI)

SPI is an exact method for depth estimation using Oasis Montaj^{TM} software. Negative values in the SPI grid image and legend colours (Fig 4.14) depict the depths of buried magnetic bodies, which maybe deep seated basement rocks or near surface intrusive. The light purple colour generally indicates the areas occupied by shallow magnetic bodies while the deep blue colour depicts areas of deep lying magnetic bodies. The SPI depths range from - 472.3 m (Shallow magnetic bodies) to - 6051.8 m (deep lying magnetic bodies)

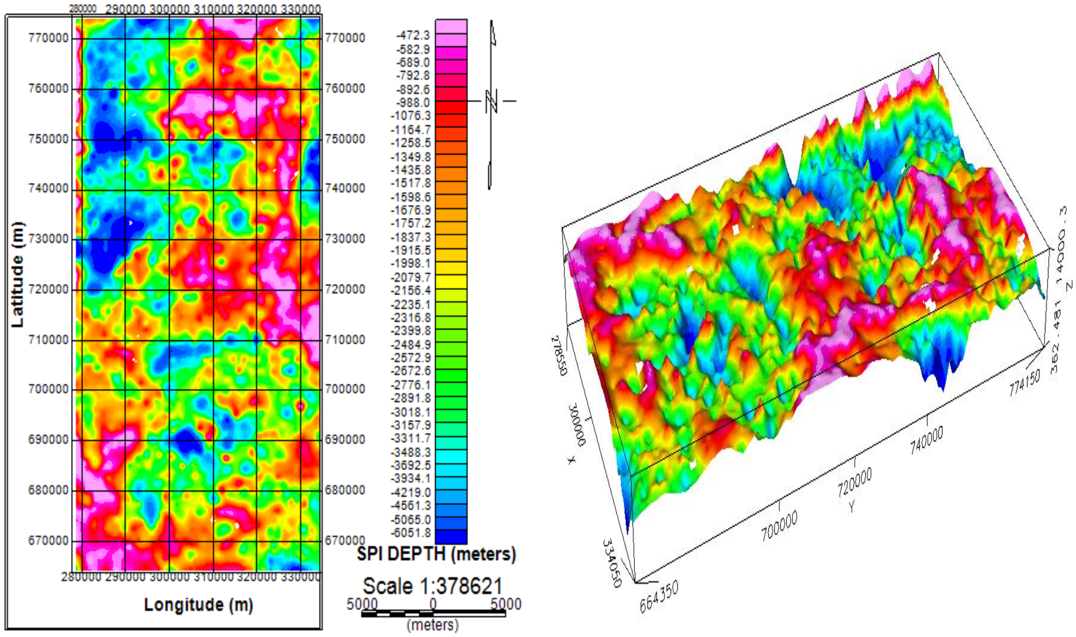

(a) (b)

Figure 4.14: SPI Grid Map (a) 2D and (b) 3D of the Study Area

4.2.3 Forward and Inverse Modeling Results: The software used for the forward and inverse modelling of the anomalies over the study area was Oasis Montaj version 4.0 which contains potent software or platform. It provides a highly interactive 3-D environment that among other applications is well suited for detailed ore body modelling for mineral exploration. To interpret our data, six profiles were taken at different parts of the study area and modeled using Potent software (Fig. 4.15). In this modeling on which profiles were taken, each profile is expected to have a degree of strike, dip and plunge where the observed values matched well with the calculated values. In Figures 4.16 – 4.21, the blue curves represent the observed field, while the red curves represent the calculated field. Because the forward modeling is a trial and error method, we adjust the physical property (susceptibility, shape and position) so that we can fit the observed and calculated field to match well. A RMS value of less than 5 was set as an acceptable error margin. The field of the model is then calculated using potent software. The summary of modeling results is shown in Table 4.4.

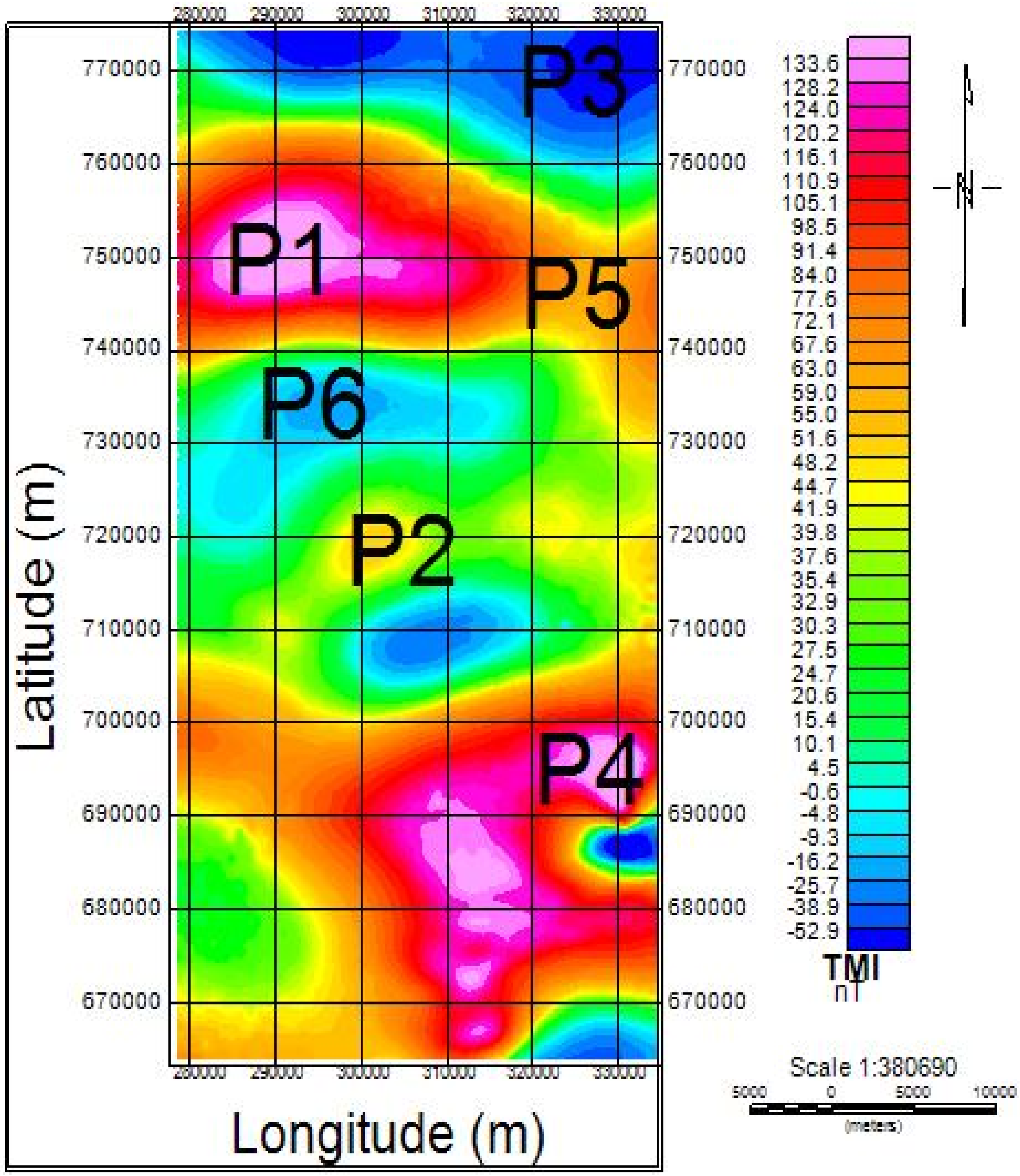

Figure 4.15: The TMI Curve with selected Profiles

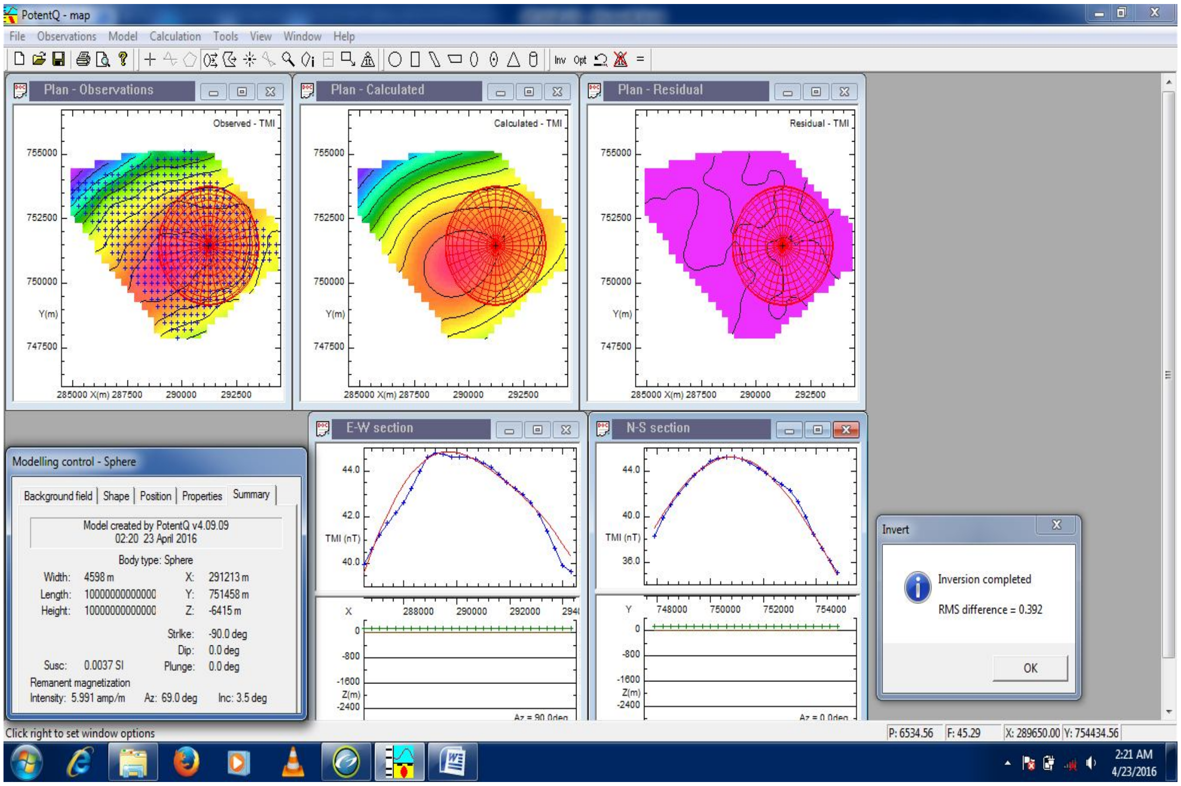

Figure 4.16: Model (Sphere) Result for Profile 1

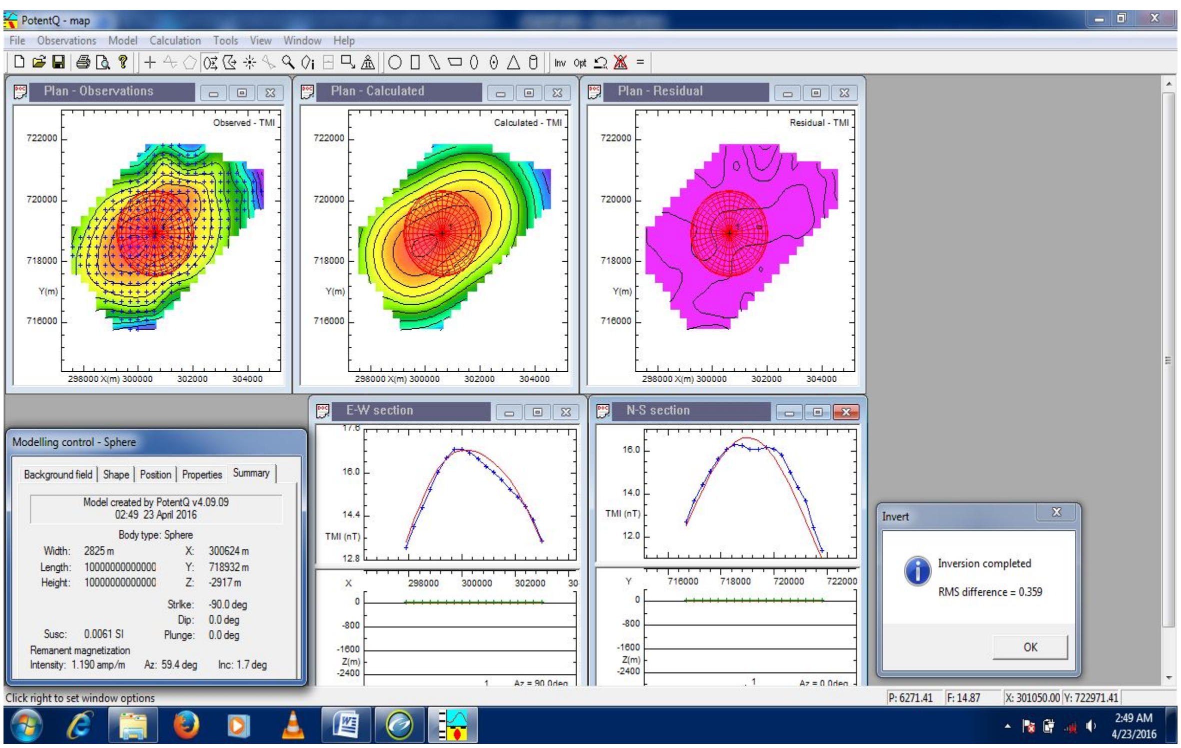

Figure 4.17: Model (Sphere) Result for Profil 2

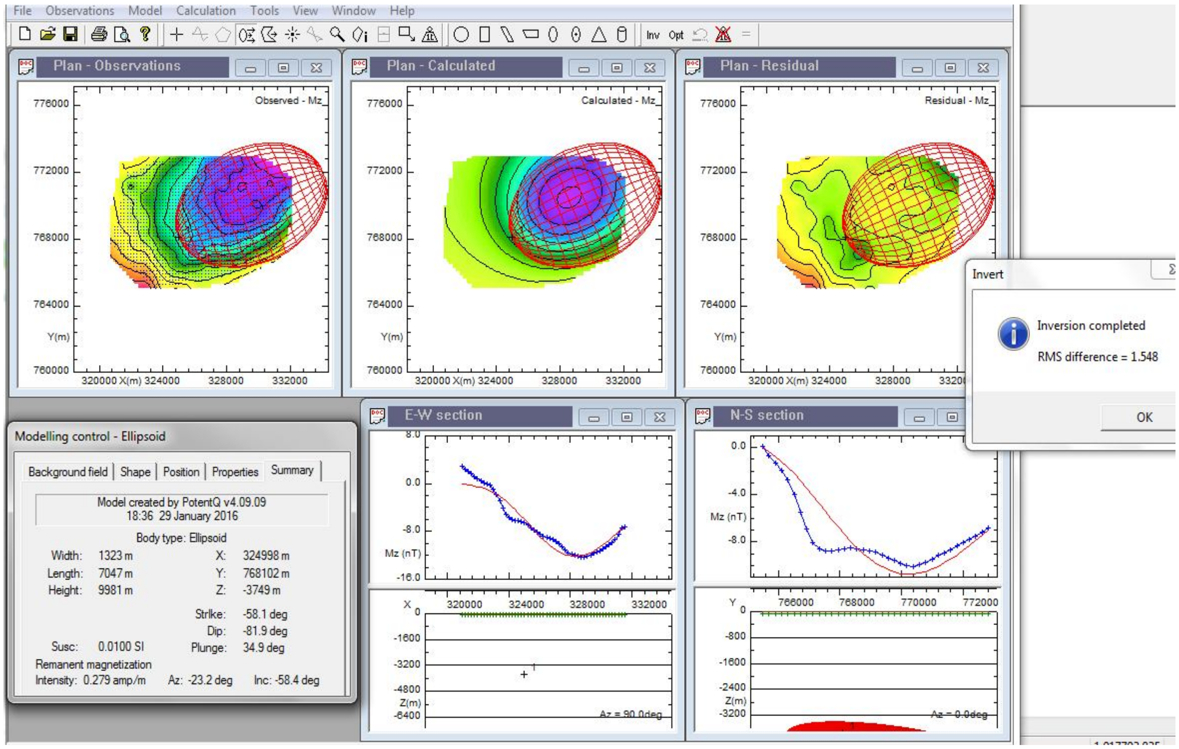

Figure 4.18: Model (Ellipsoid) Result for Profile 3

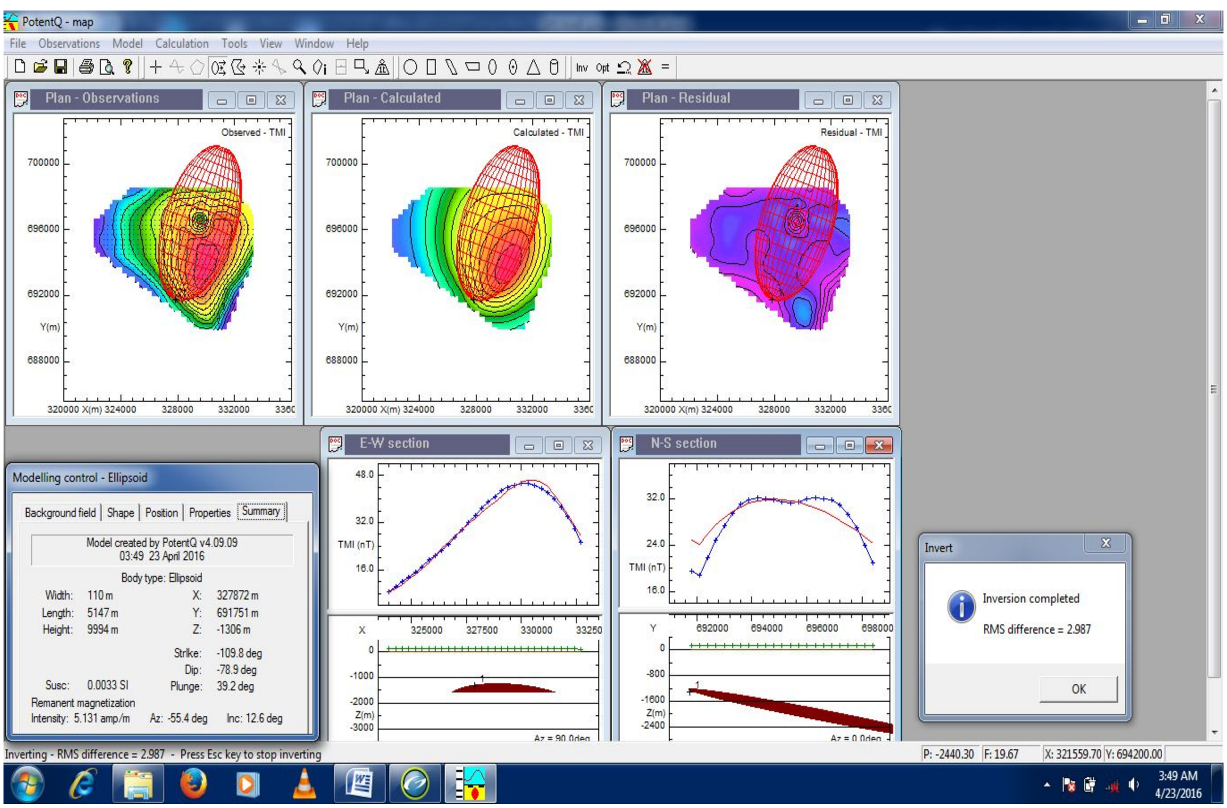

Figure 4.19: Model (Ellipsoid) Result for Profile 4

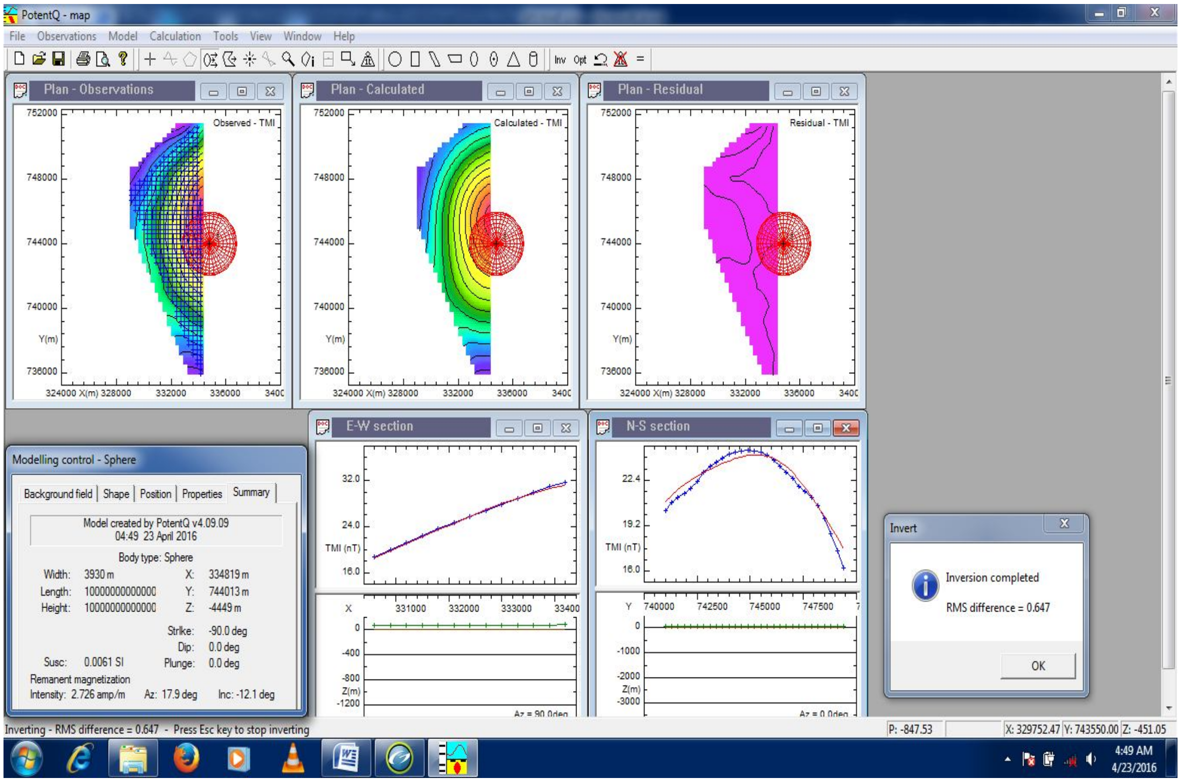

Figure 4.20: Model (Sphere) Result for Profile 5

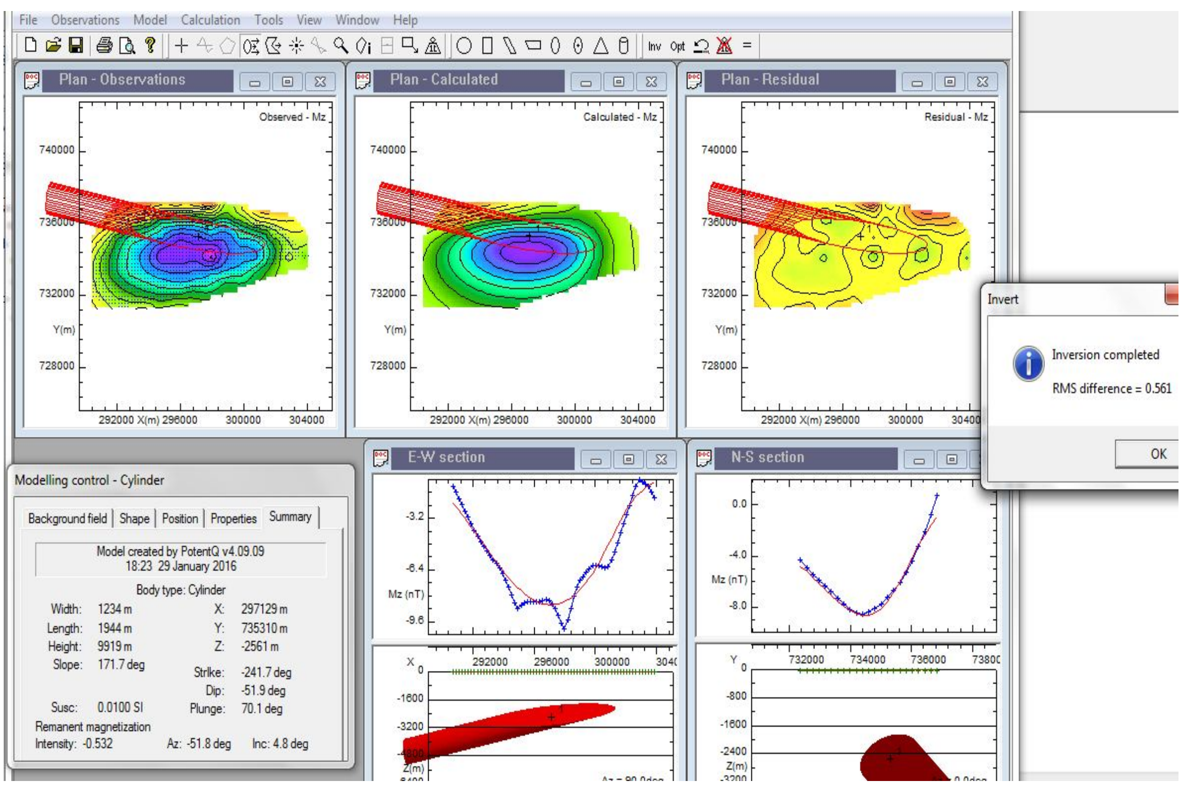

Figure 4.21: Model (Cylinder) Result for Profile 6

Table 4.4: Shows the Summary of Forward and Inverse Modeling Result.

Model	X(m)	Y(m)	Depth(m)	Dip (deg)	Plunge (deg)	Strike (deg)	Body Type	K value (SI)	Mineral Present
P1	291213	751458	-6415	0.0	0.0	-90	Sphere	0.0037	Quartzite
P2	300624	718932	-2917	0.0	0.0	-90.0	Sphere	0.0061	Hematite
P3	324998	768102	-3749	-81.9	34.9	-58.1	Ellipsoid	0.0100	Calcite and Quartz
P4	327872	691751	-1306	-78.9	-109.8	39.2	Ellipsoid	0.0033	Quartzite
P5	334819	744013	-4449	0.0	0.0	-90.0	Sphere	0.0061	Hematite
P6	2971297	735410	-2561	-51.9	70.1	-241.7	Cylinder	0.0100	Calcite and Quartz

4.3 Discussion of Result

From the TMI curve (Fig 4.1), it is seen that TMI anomaly values vary from – 110 nT to 140 nT, while the residual values are from – 150 nT to 120 nT in Figure 4.6. The colour legend bar helps to reveal area of low and high TMI values which may be attributed to variations in depth, differences in magnetic susceptibility, and differences in lithology or degree of strike. The map highlights the high amplitude anomalies which can be seen in the southeastern and northwestern parts of the study area. Low amplitude anomalies are found in the north central part of the study area. The TMI contour map drawn at intervals of 10 nT also reveals the trends of the magnetic signatures within the area. It shows that circular contours are associated with spherical anomalies within some low TMI regions of the study area and long narrow patterns which are associated with dyke – like anomalies within the north region of the study area. The result from the spectral analysis as shown in Figure 4.9 – 4.11 (cells 1 – 18) and Table 4.3, has it that the depth of the shallower magnetic sources vary from 314 to 1061 m with an average value of 632.3 m, whereas the depth of the deeper magnetic sources vary from 1465.9 to 5888.7 m with an average value of 3260.4 m. Figures 4.12 and 4.13 were produced in colour aggregate as indicated by the legend and places having blue colour corresponds to the deeper depth, areas with white colour depicted to be the average depth and the places with dust colour depicts the lowest depth.

From the forward and inverse modeling (Figs 4.16 – 4.21), the blue curves represent the observed field while the red curves represent the calculated field or the theoretical curves of the model. Their fit is measured by their visible superposition and the root mean square (RMS) values. The sub profiles in each model shows the variations of the field values with distance at the area or points modeled. The modeled results (Table 4.4) show that most of the profiles fitted more with Sphere, Ellipsoid and cylinder. These are indication of stratigraphic structures such as anticlines, diapers and faults. Results of the Forward and inverse modeling depths are 6415 m, 2917 m, 3749 m, 1306 m, 4449 m and 2561 m for profiles 1 – 6 respectively. The susceptibility values obtained from the model profiles 1 – 6 are 0.0037, 0.0061, 0.0100, 0.0033, 0.0061 and 0.0100 respectively which according to Telford *et al.* (1990) represent Quartzite, Hematite, Calcite and Quartz; and are typically sandstones and ironstones or oxides of iron which are magnetic in nature.

The depths obtained from SPI (Fig 4.14) ranges from 472.3 m to 6051.8 m. The maximum depth of 6051.8 m obtained from SPI is comparable with the maximum depth of 5888.8 m obtained from spectral analysis.

The depths obtained from the analyzed data strongly support an intrusion scenario at depth of about 6000 m or 6 km. The depth results obtained are in agreement with the results of some previous workers. Onwuemesi (1997) used spectral analysis on Anambra Basin and obtained a depth range between 0.9 and 5.6 km which is in agreement with the depth value obtained in this work using spectral analysis. Onu *et al*. (2011) used spectral analysis in lower Benue trough and got a deeper depth value of 0.518 to 8.65 km (with an average depth of 3.513 km) and a shallower depth of 0.235 km to 3.91 km (with an average depth of 1.389 km) which is higher the value obtained in this work. Obiora *et al*. (2015) worked in Nsukka area and obtained an SPI estimated depth that ranges from 151.6 m to 3082.7 m which is smaller than the depth value obtained in this work using SPI method. The maximum depth obtained by Obiora *et al*. (2015) using modeling method is 2.3 km, while in the present work, a maximum depth of 6.4 km was obtained, which is higher. The maximum depths obtained from the different methods (spectral, 5.9 km; SPI, 6.1 km; and modeling, 6.4 km) employed in this work show sufficient thick sediments favourable for accumulation of hydrocarbon which agrees with the work of Wright *et al*. (1985), which states that the minimum thickness of the sediment required for the commencement of oil formation from marine organic remains would be 2.3 km if other conditions are favourable.

CHAPTER FIVE

CONCLUSION AND RECOMMENDATION

5.1 Conclusion

The interpretation of the aeromagnetic data of the study area has been carried out qualitatively and quantitatively using Spectral Analysis, Source Parameter Imaging (SPI) and forward and inverse modeling techniques. The obtained results are in close agreement with previous works carried out in the area. The depth estimated using the three methods are comparable. The Spectral Analysis has the shallow depth in the range of 314 to 1061 m with average value of 632.3215 m and deeper depth in the range of 1465 to 5888.7 m with average value of 3260.4058 m. SPI result ranges from 472.3 m to 6051.8 m and then forward and inverse modeling depths are 6415 m, 2917 m, 3749 m, 1306 m, 4449 m and 2561 m for profiles 1- 6 respectively. Profiles 1 and 4 with susceptibility values of 0.0037 and 0.0033 depicted the presence of Quartzite in the locations, profiles 2 and 5 having a susceptibility value of 0.0061 depicted the presence of Hematite in the locations, while profiles 3 and 6 having the susceptibility value of 0.01 depicted that Calcite and Quartz are present in the locations. These geophysical/geological materials are typically sandstones and ironstones or oxides of iron which are magnetic in nature.

The modeling technique has shown that the anomalies over the study area can be modeled using spheres, Ellipsoid, and Cylinders. The results obtained were able to satisfy the objectives of this work, which includes the determination of depth to anomalous bodies, determination of depth to basement, determination of nature of anomalous bodies, susceptibility value determination and estimation of the type of mineral causing the anomaly.

5.2 Recommendation

Since this work is on aeromagnetic survey, we recommend that a gravity and ground magnetic survey of this study area should be carried out in order to affirm the obtained results in this work.

REFERENCES

Adetona A. A. and Abu M. (2013). Investigating the structures within the Lower Benue and upper Anambra Basins, Nigeria, using First Vertical Derivative, Analytical Signal and (CET) Center for Exploration Targeting Plug-in. Earth Sci. 2(5):104 – 112.

Ajakaiye, D. E. (1981). Geophysical Investigation in the Benue Trough review. Earth Evolution Sciences 2, 110 – 115.

Ajayi, C. O., and Ajakaiye, D. E. (1981). The Origin and Peculiarities of the Benue Trough: Another Look from the Recent Gravity Data in the Middle Benue. Technophysics. 80. pp. 285 – 303.

Bhattacharryya, B. K. and Leu Lei-Kuang (1975). Spectral analysis of gravity and magnetic anomalies due to two-dimensional structures. Geophysics, 40, 993 – 1013.

Bhattacharyya, B. K. and Leu Lei-Kuang (1977). Spectral analysis of gravity and magnetic anomalies due to rectangular prismatic bodies: Geophysics, 42 (1), 41 – 50.

Billings, S. D., Newsam, G.N., and Beatson, R.K. (2002). Fourier transform of geophysical data using continuous global surfaces. Geophysics, 64, 1378 – 1392.

Blakely, R. J. (1995). Potential Theory in Gravity and Magnetic Applications. Cambridge University Press, Australia.

Breiner, S. (1973). Applications Manual for Portable Magnetomaters. Geometrics. Palo Alto, California. U.S.A.

Briggs, I. C. (1974). Machine Contouring Using Minimum Curvature. Geophysics, 39 (1), 39 – 48.

Burger, H. R., Exploration Geophysics of the Shallow Subsurface, Prentice Hall P T R, 1992.

Burger R. H., Sheehan A. F. and Jones C. H. (2006) Introduction to Applied Geophysics. Published by W. W. Norton, 600 p.

Dobrin, M. B. and Savit, C. H. (1988). Introduction to Geophysical Prospecting: McGraw – Hill Inc. New York.

Ehinola, O. A., Sonibare, O. O. and Akanbi, O. A. (1985) Economic Evaluation, Recovery Techniques and Environmental Implications of the Oil Shale Deposite in the Abakaliki Anticlinorium, South Eastern Nigeria. Journal of Earth Sciences Vol.22

Ervin, C. P. (1976) Reduction to the magnetic pole using a Fast Fourier Series algorithm. Computers and Geosciences, 2, 211 – 217.

Ezema, P. O. (2004) Fundamentals of Applied Geophysics. Rojoint Communication Services Limited, Enugu Nigeria. ISBN: 978-33125-8-5.

Ezema P. O., Eze I. D., Ugwu G. Z. and Abudullahi U. A. (2014). Hydrocarbon and Mineral Exploration in Abakaliki, Southeastern Nigeria. Int. J. Eng. Sci. 3(1): 24 – 30.

Gentleman, W. M. and Sande, G. (1966). Fast Fourier transformation and profile. Prov. AFIPS 1966, Fall joint comp. Conf., 29, Spartan books New York, 563 – 578.

Gérard, A. and Griveau, P. (1972). Interprétation quantitative en gravimétrie ouagnétisme à partir des cartes transformées de gradients vertical. Geophysical rospecting, 20, 2, 459 – 481.

Gérard, A., and Debeglia, N. (1975). Automatic three-dimensional modeling for the interpretation of gravity or magnetic anomalies. Geophysics, 40, 6, 1014 – 1034.

Henderson, R. G., and Zietz, I. (1949). The Computation of Second Derivatives of Geomagnetic Fields, Geophysics, 14, 508 – 516.

Hassanien, H. I. E and Soliman, K. S. (2008). Areomagnetic Data Interpretation of Wadi Hawashiya Area for Identifying Surface Structures, North Eastern Desert, Egypt. Earth Science, 20(1): 117 – 139.

Igwesi, I. D. and Umego N. M. (2013). Interpretation of aeromagnetic anomalies over some parts of lower Benue Trough using spectral analysis technique. Int. J. Sci. Technol. Res. 2(8):153 – 165.

Ikpokonte, A. E., and Ajayi, C. O. (2003): A preliminary Interpretation of the Shallow Regional Structure deduced from Ground Magnetic Data over the Eastern Part of the Lower Benue Trough (Confluence) Area, Nigeria. Nig. Journal of Earth Sciences 2:57 – 69.

Kogbe, C. A. (1974). Paleoecologic significance of vertebrate fossils in the Dukamaje and Dange formations (Maastrichtian and Paleocene) of north western Nigeria. J. Min. Geol. 8: 49 – 55.

Ladipo, K. O.,Nwajide, C. S. and Akande, S. O. (1992). Cretaceous and Paleocene sequences in the Abakaliki and Anambra Basin, southeastern Nigeria: A field guide, international symposium on geology of Deltas. Portharcourt.

Ladipo, K. O., Ekweozor, C. and Nwajide, C. S. (2001). Geological field trip to the Anambra Basin and the Lokpanta oil shale. NAPE conference. PortHarcourt.

Lelievre, P. G. (2003). Forward modeling and inversion of geophysical magnetic data. M.sc thesis, University of British Columbia.

Likkason, O. K. Ajayi, C. O. Shemang, E. M. and Dike, E. F. C. (2005). Directional filtering and spectral analysis of aeromagnetic Data over the Middle Benue Trough,Nigeria European," Journal of Scientific Research, 2 (2) : 76 – 112,.

Lowrie, W. (1997). Fundamentals of Geophysics: Cambridge University Press, UK.

McElhinny, M. W. (1973). Paleomagnetism and Plate Tectonics. University Press Cambridge, Cambridge.

Njandjock, P. N., Manguelle-Dicoum, E., Ndougsa, M. T., and Tabod, C. T. (2006). Spectral analysis and gravity modelling in the Yagoua, Cameroon, sedimentary basin. Geofisica Internacional, 45 (2), 209 – 215.

Nwachukwu, S. O. (1975). Temperature of Formation of Vein Minerals in the Southern Portion of the Benue Trough, Nigeria. Journal of Mining and Geology 11, pp 45 – 54

Nwachukwu, S. O. (1972). The tectonic evolution of the southern portion of the Benue Trough, Nigeria. J. Min. Geol. 11: 45 – 55.

Nwajide, C. S., Reijers T. J. A. (1995). Sedimentology and sequence stratigraphy of selected outcrops in the upper cretaceous of lower Tertiary of the Anambra Basin. SPDC Exploration Report, XPMW 96007: 21 – 37.

Nuhu, G. O. (2009). Geology and Mineral. Springer Dordrecht Heidelberg London New York Library of Congress Control Number: 2009921152 © Springer-Verlag Berlin Heidelberg.

Obi, D. A., Okereke C. S., Obei B. C. and George A. M. (2009). Aeromagnetic Modeling of Subsurface Intrusives and its Implication on Hydrocarbon Evaluation of the Lower Benue Trough, Nigeria. European Journal of Scientific Research. 47 (3): 347 – 361.

Obiora, D. N., Ossai, M. N. and Okwoli, E. (2015). A case study of aeromagnetic data interpretation of Nsukka area, Enugu State, Nigeria, for hydrocarbon exploration. International Journal of Physical Sciences, 10(17): 503 – 519.

Obiora, D. N., Yakubu, J. N., Okeke, F. N., Chukudebelu, J. U. and Oha, A. I. (2016). Interpretation of aeromagnetic data of Idah area in North Central Nigeria Using Combined Methods. Journal of the Geological Society of India, 88 (1): 98 – 106.

Ofoegbu, C. O. (1988). An aeromagnetic study of part of the upper Benue Trough Nigeria. Journal of African Earth Science, 7: 77 – 90.

Ofoegbu C. O. (1984). Interpretation of aeromagnetic anomalies over the lower and middle Benue Trough of Nigeria. Geophys. J. R. Astr. Soc. 79: 813 – 823.

Ofoegbu C. O. (1985). A review of the geology of the Benue Trough, Nigeria. J. Afr. Earth Sci. 3: 293 – 296.

Okeke, F. N. (1992) Comparison of Graphical Methods of Magnetic Interpretation Based on the Interpretation of Aeromagnetic Anomaly Profiles Across the Lower Benue Trough. Nigerian Journal of Physics. 4. 103 – 113.

Onu N. N., Opara A. I., Oparaku O. I. (2011). Geological interpretation of the aeromagnetic data over the lower Benue Trough and some adjoining areas. 47th Annual International Conference of Nigerian Mining and Geoscience Society (NMGS), Programmes and Book of Abstracts. P. 43.

Onuba L. N., Audu G. K., Chiaghanam O. I. and Anakwuba E. K. (2011). Evaluation of aeromagnetic anomalies over Okigwe area, Southern Nigeria. Res. J. Environ. Earth Sci. 3(5):498 – 507.

Onuba, L. N., Onwuemesi, A. G., Anudu, G. K., Chiaghanam, O. I. and Ifelunni, C. D. (2008). Interpretation of aeromagnetic anomalies over Benue Trough, Northeastern, Nigeria. Journal of Natural and applied sciences, 9: 1 – 12.

Onwuemesi A. G. (1997). One dimensional spectral analysis of aeromagnetic anomalies and curie depth isotherm in Anambra Basin of Nigeria. J. Geodynamics. 23(2): 95 – 107.

Onwuemesi A. G. (1995). Interpretation of magnetic anomalies from the Anambra Basin of southeastern Nigeria. Ph.D thesis, Nnamdi Azikiwe University, Awka, Nigeria.

Pal, P. C., Khurana, K. K., and Unnikrishnan, P. (1978). Two examples of spectral approach to source depth estimation in gravity and magnetic. Pure Applied Geophysics, 21: 772 – 783.

Petters S. W. (1978). Stratigraphic Evolution of the Benue Trough and its implications for the Upper Cretaceous Paleogeography of West Africa. J. Geol. 86(3):11 – 322.

Reyment, R. A. (1965). Aspects of the Geology of Nigeria- The Stratigraphy of the Cretaceous and Cenozoic deposits. University of Ibadan Press. Ibadan.

Revees, C. (2005). Aeromagnetic Surveys; Principles, Practice and Interpretation. GEOSOFT.

Robinson, E. S., and C. Coruh, (1988). Basic Exploration Geophysics, John Wiley,

Sharma, P. V. (1987) Magnetic Method Applied to Mineral Exploration Ore. Geol. Rev, 2: 323 – 357.

Spector, A. and Grant, F. S. (1970). Statistical models for interpreting aeromagnetic data. Geophysics, 35, 293 – 302.

Tadjou, J. M., Nouayou R., Kamguia J., Kande H. L. and Manguele-Dicoum E. (2009). Gravity analysis of the boundary between the Congo Craton and the Pan-african belt of Cameroon. Austrian journal of earth sciences, 102, 71 – 79.

Telford W. M., Geldart L. P., Sheriff R. E. (1990). Applied Geophysics. 2nd edition. Cambridge University Press, Cambridge.

Thurston, J. B. and Smith, R. S. (1997). Automatic Conversion of Magnetic Data to Depth, Dip and Susceptibility Contrast Using the SPITM Method. Geophysics. 62: 807 – 813.

Thurston, J. B., Smith, R. S. and Guillon, J. C. (2002). A multimodel method for depth estimation from magnetic data: Geophysics, 67, 555 – 561.

Whiteman, A. J. (1982). Nigeria: Its Petroleum Geology, Resources and Potentials 1, 176pp; 2, 238pp. Graham and Trotham Limited: London, UK.

Wightman, W. E., Jalinoos, F., Sirles, P., and Hanna, K. (2003). Application of Geophysical Methods to Highway Related Problems. Federal Highway Administration, Central

Federal Lands Highway Division, Lakewood, CO, Publication No. FHWA-IF-04-021.

Wright J. B. (1976). Origins of the Benue Trough – a critical review. In: Geology of Nigeria, eds. Kogbe CA. Elizabethan Publ. Co. Lagos. pp. 309 – 318.

Wright J. B., Hastings D., Jones W. B. and Williams H. R. (1985). Geology and Mineral resources of West Africa. George Allen and Urwin, London.